# INVESTIGATION OF MICROCHANNELS HEAT EXCHANGERS FOR CONDENSERS

**A Thesis Submitted to**
**the Graduate School of Engineering and Science of**
**İzmir Institute of Technology**
**in Partial Fulfillment of the Requirements for the Degree of**

**MASTER OF SCIENCE**

**in Energy Engineering**

**by**
**Furkan Tuğberk SEVENCAN**

**March 2021**
**İZMİR**

# ACKNOWLEDGMENTS

Firstly, I would like to thank my advisor Assoc. Prof. Dr. Erdal ÇETKİN for his continuous support and the inspiring subject that my thesis is about.

I also thank my classmate Serkan EROL, Emre AYDENİZ and İsmail Gürkan DEMİRKIRAN for their support during the courses I have taken during the Master of Science (MSc).

Finally, I am thankful to my mother Nurten KURUMAHMUT SEVENCAN, my father Ayhan Ogün SEVENCAN and my sister Ahsen Hazal SEVENCAN for their limitless support and encouragement. I am also thankful to my uncle Ali Paşa KURUMAHMUTOĞLU.

# ABSTRACT


## INVESTIGATION OF MICROCHANNELS HEAT EXCHANGERS FOR CONDENSERS

There are limited types of condenser types/designs in the market although there are many distinct heat exchangers available. One reason is related to the complexity of the phase-change mechanism and how it is affected by the geometric parameters of the heat exchanger. Technological requirements force the size of any component to become smaller and condensers are no exception for this trend. However, there is a limit for scaling down the current condensers, and their compactness cannot be decreased due to their serpentine design. The transition from serpentine designs to parallel microchannels is promising as the required coolant volume would decrease significantly for the same cooling due to enhanced heat exchange surface area. However, parallel channel designs are challenging to implement due to irregularities in pressure distribution which would yield phase change and condensation temperature significantly. In the present thesis, a microchannel heat exchanger was selected and the imperfections related to the pressure distribution irregularities were progressively developed numerically. Geometrical parameters were optimized to eliminate the flow maldistribution resulted from non-homogeneous pressure distribution in the condenser. The effects of header shape (from rectangular to tapered) on flow uniformity are not dramatic. Then, manifold channels were relocated with given protrusion depths which were optimized using an iterative approach. Relocating the channels enables the pressure uniformity. Finally, the condensation behavior of the design developed with the aim of enabling uniform flow resistance was documented. Under the given operational conditions, three different height channel design is 100% condensed R410a from the vapor phase into the liquid phase. A and B design were condensed the refrigerant fluid in a low Reynolds number meanwhile, C design was condensed in a high range of Reynold number. All in all, effects of maldistribution on flow regime were tried to be eliminated with new geometric design approaches and condensation effect in new geometries was able to be seen 100% at low flow rates.



***Keywords:*** *Channel Protrusion Depths, Condensation Effect, Flow Irregularities, Maldistribution, Microchannel Heat Exchangers.*

# ÖZET

## YOĞUŞTURUCULAR İÇIN MİKROKANALLI ISI DEĞİŞTİRGEÇLERİNİN ARAŞTIRILMASI

Günümüzde termal sistemlerin çoğunda kullanılan ısı değiştiricilerinin piyasada birçok farklı türü bulunmakla birlikte az sayıda kısmı yoğuşturucu olarak kullanılmaktadır. Teknolojinin ilerlemesiyle birlikte cihazların küçülme eğilimi, ısı değiştiricilerinin de günden güne daha kompakt hale gelmesini sağlamıştır. Mevcut yoğuşturucuları ölçeklendirmek için bir sınır vardır ve serpantin tasarımları nedeniyle boyutları daha fazla azaltılamaz. Serpantin tasarımlarından paralel mikro kanallara geçiş, artan yüzey alanı nedeniyle aynı soğutma için gerekli soğutma sıvısı hacminin büyük ölçüde azalacağı için umut vericidir. Bununla birlikte, paralel kanal tasarımı, büyük ölçüde faz değişimi ve yoğunlaşma sıcaklığına neden olacak basınç dağılımındaki düzensizlikler nedeniyle uygulanması zordur. Bu çalışmada, bir mikro kanallı ısı eşanjörü seçilmiş ve basınç dağılımı düzensizlikleri ile ilgili kusurlar sayısal olarak aşamalı olarak giderilmiştir. Yoğuşturucudaki homojen olmayan basınç dağılımı sonucu oluşan akış düzensizlikleri geometrik parametreler kullanılarak optimize edilmiştir. Dikdörtgen formda olan ısı değiştiricisinin manifoldunun konik forma çevrilmesiyle akış düzensizliğinde küçük bir etki görülmüştür. Başka bir yaklaşım olan manifoldun içindeki kanalların yeniden konumlandırılma uygulaması yapılmıştır. Yeniden konumlandırma sonucu oluşan çıkıntı derinliği seri denemelerin sonucunda optimum hale getirildi ve bunun akış dağılımına yoğun etki gösterdiği gözlemlenmiştir. Çalışmada seçilen değerler sonucunda akışkanın %100'ü, buhar fazından sıvı fazına yoğunlaştığı gözlemlenmiştir. A ve B tasarımları düşük Reynolds sayılarında %100 yoğuşma sağlarken C tasarımı daha geniş Reynolds sayılarında da yoğuşma sağlamaktadır. Sonuç olarak, akış bozukluğunun akışa olan etkisi yeni geometrik tasarım yaklaşımlarıyla ortadan kaldırılmaya çalışılmıştır ve yeni ısı değiştiricisi geometrisinde yoğuşma etkisi düşük debili akışlarda %100 oranında görülmüştür.

***Anahtar Kelimler:*** *Mikro Kanallı Isı Değiştiricileri, Akış Bozuklukları, Kanal Çıkıntı Derinlikleri, Yoğuşma Etkisi*

# TABLE OF CONTENT

# LIST OF TABLES

**Table** **Page**

# LIST OF FIGURES

**Figure** **Page**

# LIST OF SYMBOLS

| | | |
|---|---|---|
| μ | Dynamic Viscosity | kg/(m.s) |
| ρ | Density | $kg/m^3$ |
| C | Turbulent Dissipartion Rate | J/(kg.s) |
| D | Diameter | mm |
| V | Velocity | m/s |
| μm | Micrometer | $10^{-3}$mm |
| *u,v* | Velocity Component | m/s |
| α | Volume | $m^3$ |
| Coeff | Coefficent | |
| T | Temperature | °C |
| h | Entalpy | J/kg |
| Q | Transferred Heat | J |
| $\dot{m}$ | Mass Flow Rat | kg/s |
| A | Cross Section Area | $mm^2$ |

# CHAPTER 1

# INTRODUCTION

Human beings have used heat in many different fields as an energy form for their needs. With the rising industrial needs and increasing production techniques, mankind has discovered many different devices and developed these devices in line with their needs. In the modern age, heat exchangers are used in many areas to manage heat by different types of heat exchangers. With the increasing demand for controlled conditions, exchangers are more specific and varied. Heat exchangers have been used in the chemical, petrochemical and end-user industries. While the heat exchangers used in the heavy industry enable large and high-capacity heat transfer, the heat exchangers used for microchips in the electronics industry require considerable heat transfer from very small areas. At the same time, HVAC systems have heat exchangers used as condensers for cooling purposes to meet the comfort of life and food needs. This diversity has kept the investment in heat exchangers and the need for research up to date.

Today, the global heat exchanger market is growing in line with the industry's needs and continues to evolve in line with environmental concerns. In the last decade, the market's annual compound annual growth rate was 6.5% and the market size was projected to cross $20,5 billion by 2020. Assessed in the end-user category, the chemical petrochemical industry, HVAC and the refrigeration industry had a 29.2% share in 2020, the highest level in its history. In the light of technological developments, the trends of heat exchangers in the market are made more compact to meet the demand in the market and reduce the damage to the environment by increasing efficiency (Prescient&Strategic Intelligence, 2016).

Basically, the heat transfer is proportional to the surface area although during the last decades, reducing material usage while increasing energy efficiency and the space limitation have led to an obligation to improve heat and mass exchangers. More than 40 years of research has brought on initiatives, such as reducing the volume and size of

energy exchange. Micro-channels have been the revolutionary development with various methods based on recent intensive research.

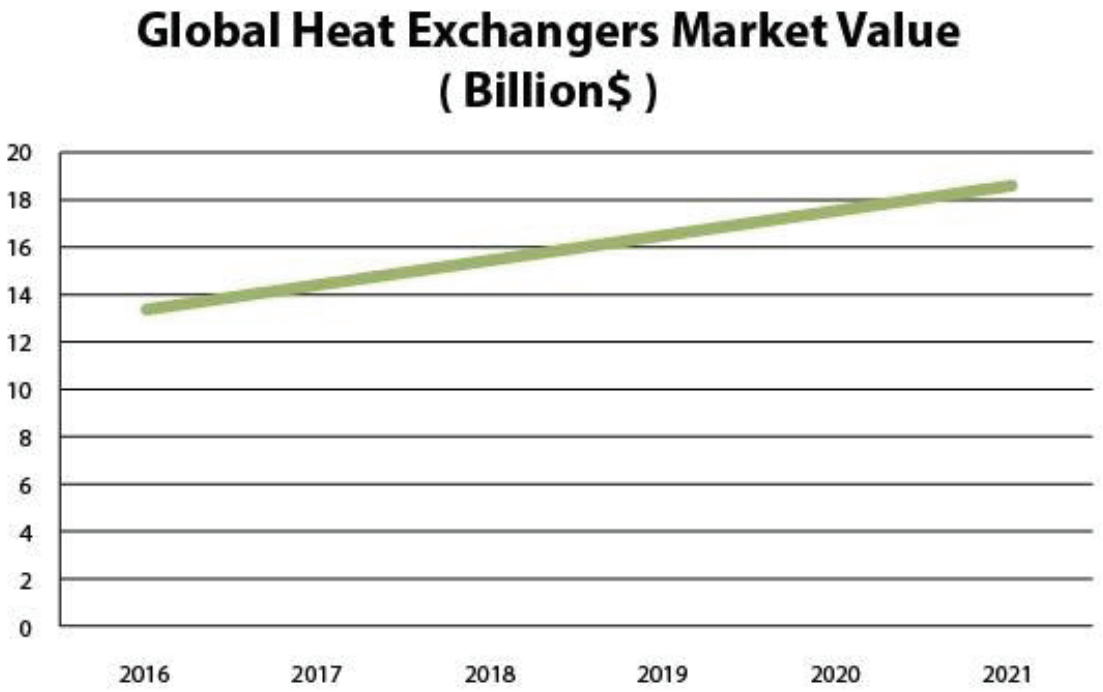


Figure 1.1 Global heat exchanger value (Source: Gosreports, 2017)

Appropriate design and convenience of micro-channels on correct subjects revealed that high surface-area-to-volume ratios reached quite high heat transfer coefficients. Concurrently, pressure drops between the channels may reduce these coefficients and flow irregularities may occur accordingly. It has also been recorded that it reduced the flow circulation within the channels. All in all, these results displayed that micro-channels have been among the most trustworthy studies to tackle the issues reported above. Current studies suggest that the utilization of micro-channels in diverse industries may avail more than today and can lead to new revolutions. As a result, production costs are gradually decreasing, and solutions to these elements, which are the main constraints of micro-channels, continue to find answers quickly. Thus, to examine all these developments and advancements, we need to separate heat exchangers according to their types and ways of working.

## 1.1 Background

Heat exchangers can be classified in two different ways as follows: Classification according to flow configuration (Figure 1.2) and classification according to construction (Figure 1.3).

There are four basic configurations for heat exchangers: namely countercurrent flow, cocurrent (parallel) flow, crossflow, and hybrid flow.

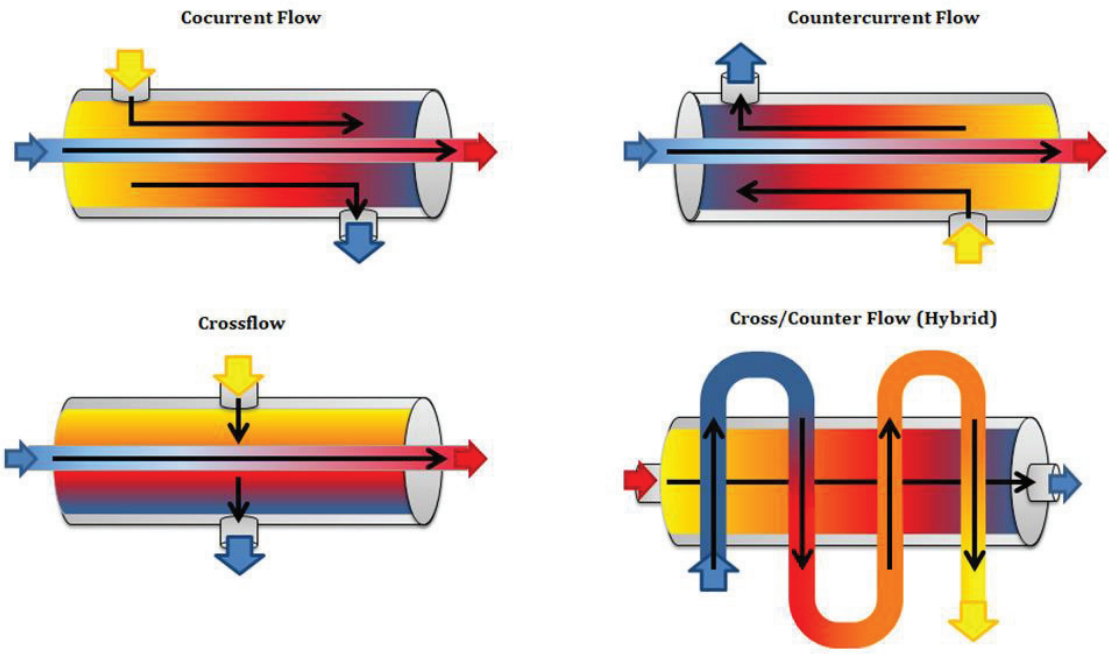


Figure 1.2 Heat exchanger classification by flow configurations Source: Ronquillo, 2020)

These configurations can be expressed as follows: Concurrent (parallel) flow has two different contactless flow paths in the same direction, otherwise is the countercurrent flow and the crossflow indicates a flow path direction perpendicular to the other flow path. The hybrid flow can be defined as mixture of crossflow and cocurrent flow.

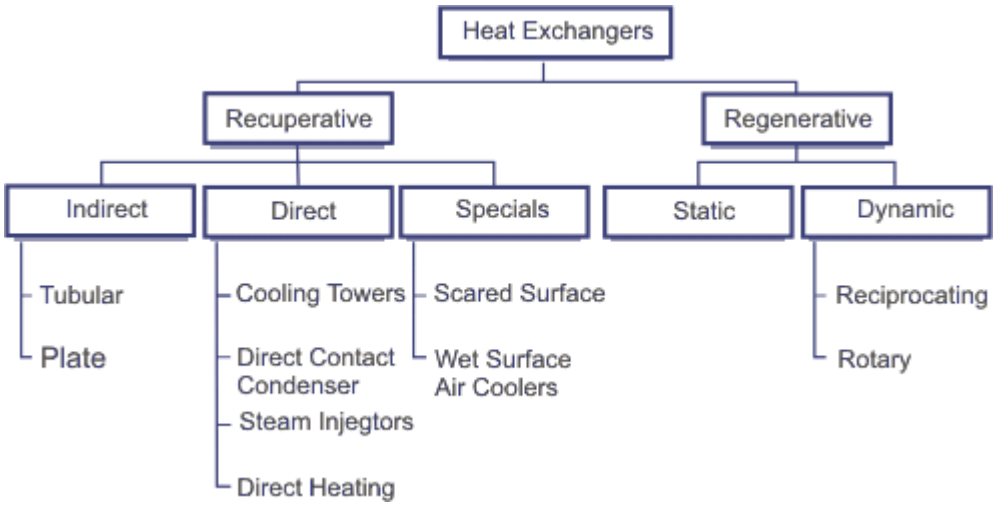


Figure 1.3 Heat exchanger classification by construction (Source: Brogan, 2011)

The heat exchangers can also be classified by construction which are Recuperators and Regenerators (Husain, 2016). All types of the recuperator and regenerative heat exchanger can be seen in Figure 1.2 and industries and applications of these heat exchangers are provided in Table 1.1. Recuperators are mostly known as surface generators which are usually made of tubes or pipes and heat is transferred through the surface of the partition wall. A basic example of recuperative heat exchangers includes car radiators, condensers and oil coolers. Regenerator-type of heat exchangers can be classified into direct contact and indirect contact.

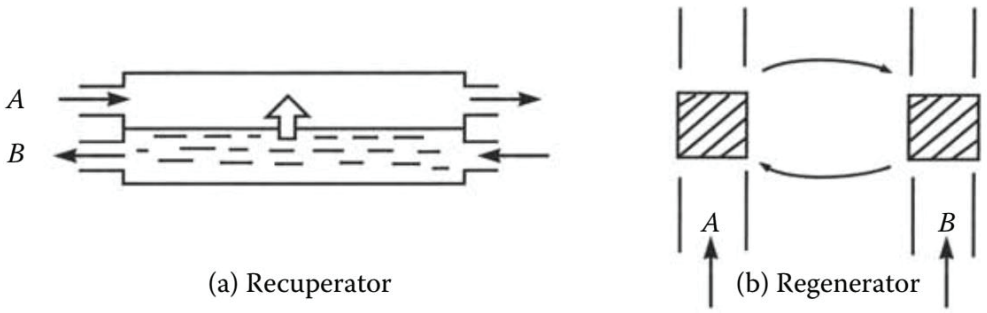


Figure 1.4 Recuperator & Regenerator (Source: Kakaç, Hongtan, & Anchasa, 2012)

In a regenerative heat exchanger, alias capacitive heat exchanger, the fluid flows into the heat exchanging path, which could be cold or hot, then the other fluid passes through the same path. The exchanging area can be named by a matrix absorbed or released the heat to the second fluid. If hot fluid passes, then it is called hot blow; if cold fluid passes, then it is called cold blow. The regenerator heat exchanger can be sort

of two categories: static and dynamic. Thus, the heat exchange on both categories is transient and considerable care should be taken in their design.

Table 1.1. Industries and application of heat exchangers by type (Source: Brogan, 2011)

| Type of Heat Exchanger | Common Industries and Applications |
|---|---|
| Shell and Tube | · Oil refining<br>· Preheating<br>· Oil cooling<br>· Steam generation<br>· Boiler blowdown heat recovery<br>· Vapor recovery systems<br>· Industrial paint systems |
| Double Pipe | · Industrial cooling processes<br>· Small heat transfer area requirements |
| Plate | · Cryogenic<br>· Food processing<br>· Chemical processing<br>· Furnaces<br>· Closed loop to open loop water cooling |
| Condensers | · Distillation and refinement processes<br>· Power plants<br>· Refrigeration<br>· HVAC<br>· Chemical processing |
| Evaporators/Boilers | · Distillation and refinement processes<br>· Steam trains<br>· Refrigeration<br>· HVAC |
| Air Cooled/Fan Cooled | · Limited access to cooling water<br>· Chemical plants and refineries<br>· Engines<br>· Power plants |
| Adiabatic Wheel | · Chemical and petrochemical processing<br>· Petroleum refineries<br>· Food processing and pasteurization<br>· Power generation<br>· Cryogenics<br>· HVAC<br>· Aerospace |
| Compact | · Limited space requirements (e.g., aircraft and automobiles)<br>· Oil cooling<br>· Automotive<br>· Cryogenics<br>· Electronics cooling |

The recuperative heat exchangers can be categorized into three main groups, which are indirect, direct and specials. The recuperative heat exchangers have different flow paths for each flow at the same time. Today, most of the heat exchangers are in these three categories. In Table 1.1 below, some of the heat exchangers types and industries or applications in which they were used are listed.

Microchannel heat exchangers have ordinarily parallel channels with less than 1 mm hydraulic diameter Kandlikar & William J. Grande, (2003). Simply, parallel channels improve the transport and distribution of fluid. Multiple parallel channels are used for different purposes, such as to enhance the heat exchange, mass transfer in absorbers.

Just because of the advantages of microchannel heat exchangers, many researchers have focused on the development of these devices and overcoming ongoing problems. For that purpose, Vist & Pettersen, (2004) conducted an experimental study to find out how varying operational factors and geometrical factors influenced two-phase distribution in a compact heat exchanger. The experimental setup was based on an automobile evaporator with a cooling capacity of 5 kW. Refrigerant fluid (R134a) was distributed into 10 channels of the heat exchanger. In their study, two types of manifold were used (ID8 and ID16 with 8 mm diameter and 16 mm diameter, respectively) for headers. The findings obtained indicated that vapor phase flows were distributed into an adjacently located upward flow liquid phase; flow was distributed evenly in the last tube of the heat exchanger. For downward flow, opposite effects were observed. When the vapor fraction increased at the inlet of manifold, both flow experiments yielded better distribution and limited the differences between 8mm and 16mm diameter manifolds.

The first main disadvantage of a microchannel heat exchanger is flow distribution. Many studies and researchers have worked on this disadvantage and tried to change some parts of the heat exchangers and altered the design of header, channel and fins. For example, A.Gogulakrishnanan & M.Arun Pranesh, (2016) performed a numerical and experiment study on maldistribution and cross-sectional shape of heat exchangers. The design of the numerical study was a dimensional model that was created and meshed by GAMBIT modeling software. Model lateral pipe dimensions were 16x1.03x125mm. The analysis was conducted on the circular and square cross-

sectional shape of the header. The governing flow equations were continuity equations and momentum equations. This analysis was used for the standard k-ε turbulence model. The dissipation rate constants were $C_{1\varepsilon}$, $C_{2\varepsilon}$, and $C_{3\varepsilon}$ . Fluid or both mixtures (liquid and gases) can be modeled by solving energy, momentum and continuity equations. The coolant was chosen to regulate the temperature of the system. The second-order upwind and finite volume method was adapted using a coupled solver for momentum and continuity equations. Given the findings obtained in this study, the square cross-section header yielded a better flow distribution as than the other inflexible cross sections. The flow distribution was influenced by the header shape. The result of CFD analysis showed that maldistribution was closely related to operational conditions and geometrical shapes of the header. The experimental work was established in light of the results of CFD analysis conducted using geometrical parameters of the header and channels. Microchannel heat exchanger channels have a gap in millimeter level for fluid flow. When the scale of channels was increased to centimeter-level, the same header design effects are also seen on flow distribution. For example, to investigate such effects, Jafar M. Hassan & Thamer A. Mohamed, (2014) conducted a numerical and experimental study to find out the uniformity of the flow distribution in various types of manifolds. The numerical study used Fluent for a solver CFD software and Gambit for a Mesher software. The model was meshed with 1000000 elements and the turbulent k-ε model was chosen for flow configuration. Three tests were performed on CFD and each test's Reynolds number was $10x10^4$, $15x10^4$ and $20x10^4$, respectively. The inlet water temperature was 20°C and it was valid for all tests. The numerical model was validated by the experimental model and the results were close and acceptable. The results of CFD showed that the optimum design of a tapered manifold was attained when the diameter ratio was two ($D_1/D_2$). The experimental study was established with longitudinal and tapered manifolds. Each manifold had five branches with the same diameter and the same size (150x150) shallow tank to collect the water. Six piezometers were set up uniformly to gauge pressure. Their findings revealed that some maldistribution occurred in circular cross-section header and tapered cross-section header had more uniform distribution.

Flow distribution in headers largely depends on where the headers are used for combining or dividing and which conditions are prepared for the headers. The afore-mentioned study used the headers for dividing and the experimental setup was prepared

as open flow. Therefore, the Reynolds number slightly affected the flow distribution. However, if the model were built as a closed system, the Reynolds number would have significant effects on flow distribution. Kim, Eunsoo Choi, & Young I. Cho, (1995) presented a study to investigate the effects of Reynolds number and header shape on flow distribution using a liquid cooling module in a parallel flow manifold. They literately found that pressure difference highly influenced the flow distribution in manifolds. Their study aimed to modify the header shape to obtain a more desirable flow distribution. To achieve that, three different header shapes (rectangular, triangular, and trapezoidal) were used in the numerical study. Reynolds number was chosen as between 50 to 300 and defined as $\frac{\rho V_{in} D}{\mu}$, where $V_{in}$ was incoming flow at the dividing header. FIDAP was used as a solver, and the total grid was 192x128. After numerical analysis, the result showed that header shapes and Reynolds number had significant effects on flow distribution in a manifold. In the last channel, the inertia effect was encountered in the manifold. This fact significantly decreased in the triangular shape and trapezoidal shape headers. Although Reynold's number was a function of the flow distribution, the percent flow rate increased in the last channel with increasing Reynolds number. However, non-uniformity increased when the Reynolds number was higher. The static pressure difference is a direct consequence of flow distribution in a manifold between dividing and combining headers. The main trend of pressure is one that decreases along the direction of downstream in the dividing and combining headers. The combining header has a more stable pressure profile than the dividing header. When it turns into the channel, the flow stalls on the baffle walls in the dividing channel. Pressure difference was almost uniform between dividing and combining headers channel in the triangular headers. The result of study showed that the flow distribution was largely dependent on the Reynolds number and shape of headers and the triangular header presented the best flow distribution regardless of the Reynolds number.

## 1.2 Motivation

The constructal theory suggests that the formation of flow structures (e.g., river basins, lungs, atmospheric circulation and vascularized tissues) that were seen

throughout nature can be justified based on an evolutionary principle, such as the increase in flow access over time. The theory statement shows that the generation of flow configurations was a universal phenomenon in all physics and was covered by the laws of physics. This law is related to the necessity of design and the time direction of the phenomenon: When the videotape of the design evolution "movie" runs, the existing configuration is replaced by a configuration that is easier to flow globally. The constructal law has two useful aspects: the prediction of natural phenomena and the strategic engineering of a new type of building based on the law of construction, that is, not imitating nature (Bejan & Lorente, 2010). With recent improvements in computational fluid dynamics software and more powerful personal computers, CFD solutions have become more significant tools in providing solutions for flow distribution. The last study mentioned above was based on a CFD solution before the settings of experimental research using CFX, OpenFOAM, Fluent, CFD-Ace and STAR-CCM+ software.

In the present study, a 2D micro-channel heat exchanger was modeled using Ansys Fluent CFD software to have better flow distribution. Constructal design theory approaches were used and channel protrusion changed iteratively for uniform flow distribution in the header. The uniform design was also performed using the refrigerant fluid of r410a under different inlet and outlet conditions. Effects of different Reynolds numbers on heat exchange and flow distribution were also investigated.

# CHAPTER 2

# DEFINITION AND ANALYSIS DESIGN PARAMETERS

## 2.1 Fundamentals of Microchannel

Tuckerman & Pease, (1981) first suggested and used the idea of the micro-channel heat exchanger. Mehendale S.S, Jacobi A.M., & Shah R.K. , (1999) describes the micro-channel heat exchanger as if the heat exchanger's hydraulic diameter was less than 1 mm. Swift, Migliori, & John, (1985) first developed with micro-channel heat exchangers for heat exchange between two different fluids.

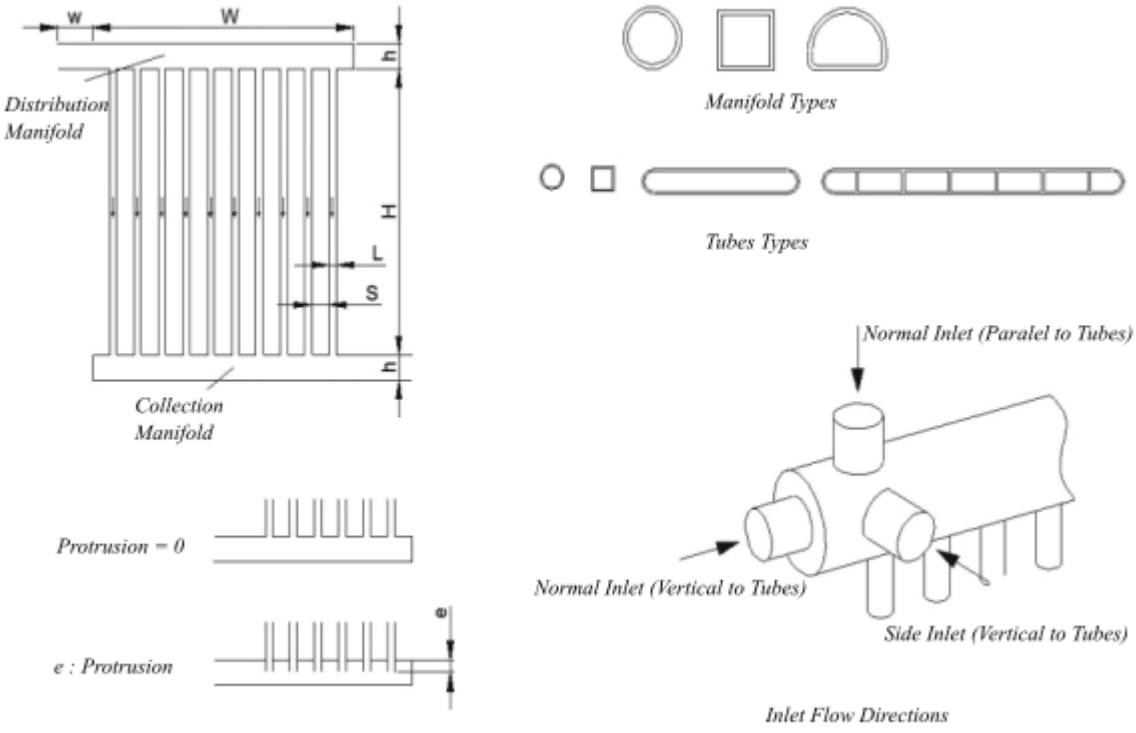


Figure 2.1. Schematics of Different Manifold and Flow Designs (Source: Dönmez & Onbaşıoğlu, 2013)

Brief description of microchannel heat exchangers is illustrated in Figure 2.1. The manifold is defined as the main flow location to the channels. T junction is the simplest manifold type that expresses an outlet or inlet in the direction perpendicular to the flow in the manifold. The channels can be defined as the flow media entering or leaving the mainline.

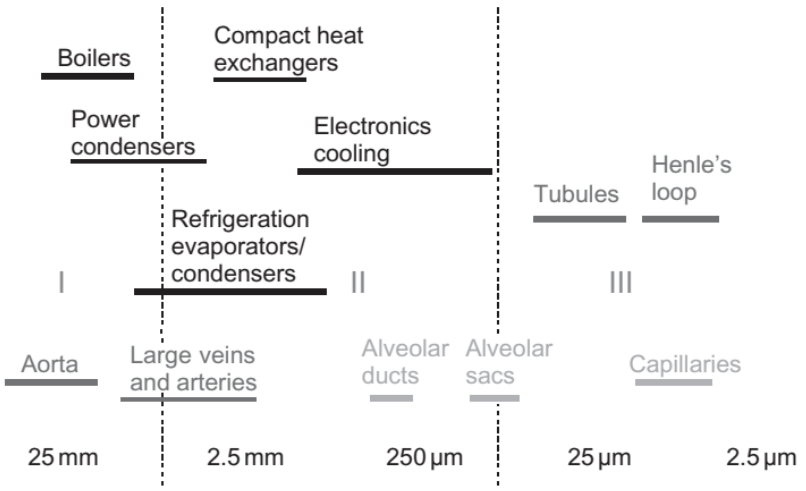


Figure 2.2. Ranges of channel diameters employed in various applications (Source: Kandlikar, Satish & Steinke, & Mark, 2003)

The ranges of channel dimensions employed in different systems are shown in Figure 2.2. While larger channels are used for fluid transport, engineers are interested in the range between 2.5 mm - 250 µm. In addition to Figure 2.2, Table 2.1 shows the channel classification used in different engineering disciplines.

Table 2.1. Channel classification scheme (Source: Kandlikar & William J. Grande, 2003)

| | |
|---|---|
| Conventional Channel | > 3 mm |
| Minichannels | 3 mm ≥ D > 200 µm |
| Microchannels | 200 µm ≥ D > 10 µm |
| Transional Microchannels | 10 µm ≥ D > 1 µm |
| Transional Nanochannels | 1 µm ≥ D > 0.1 µm |
| Nanochannels | 0.1 µm ≥ D |
| D: Smallest Channel Dimension | |

## 2.2 Flow Maldistribution in Header

As compared to uniform flow, maldistribution can be defined as defective or uneven rate of flow. Maldistributions may arise from mechanical defects, fouling/corrosion, be self-induced or two-phase flow. In short, mechanical defects include irregularities in header design, inlet duct dimensions and other manufacturing tolerances. Self-induced maldistribution includes changes in flow specifications, fluent viscosity, flow types (laminar to turbulent or the opposite), density or phase of flow (like rapid freezing). On the other hand, two-phase flow maldistributions involve two different fluid mixtures and one fluid with a different phase. Lastly, fouling/corrosion maldistribution arises from contaminated flow environments (inside or outside) (Mueller & Chiou, 1988).

In this thesis, mechanical causes and self-induced maldistribution in microchannel heat exchangers were the focus.

### 2.2.1 Two-Phase Flow

Based on the combination and interface structure, there is a variety of two-phase flows. The interfaces of two-phase mixtures can be described by the presence of one or more interfaces and discontinuities. Taking the macroscopic scale of those interfaces into consideration, four phases can be defined as: solid, liquid, gas, and plasma (ionized gas) (Pai, 1977).

As shown in Figure 2.3, two-phase flow can be divided into three major classes based on the geometry of the interfaces: separated flow, transitional or mixed flow and dispersed flow. Each class has different regimes depends on the configuration of the flow types, and every configuration has a process example.

For the condensation process while phase changing occurs, mixed or transitional flows regimes changes can be seen on the working system. After the working system reaches the steady-state conditions, film or annular flow regime changes are continuously flow in the working area.

| Class | Typical regimes | Geometry | Configuration | Examples |
|---|---|---|---|---|
| Separated flows | Film flow | 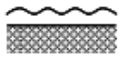 | Liquid film in gas<br>Gas film in liquid | Film condensation<br>Film boiling |
| | Annular flow | 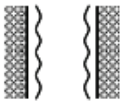 | Liquid core and gas film<br>Gas core and liquid film | Film boiling<br>Boilers |
| | Jet flow |  | Liquid jet in gas<br>Gas jet in liquid | Atomization<br>Jet condenser |
| Mixed or Transitional flows | Cap, Slug or Churn-turbulent flow | 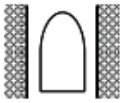 | Gas pocket in liquid | Sodium boiling in forced convection |
| | Bubbly annular flow | 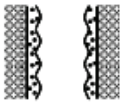 | Gas bubbles in liquid film with gas core | Evaporators with wall nucleation |
| | Droplet annular flow | 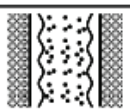 | Gas core with droplets and liquid film | Steam generator |
| | Bubbly droplet annular flow | 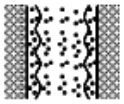 | Gas core with droplets and liquid film with gas bubbles | Boiling nuclear reactor channel |
| Dispersed flows | Bubbly flow | 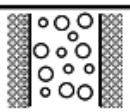 | Gas bubbles in liquid | Chemical reactors |
| | Droplet flow | 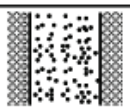 | Liquid droplets in gas | Spray cooling |
| | Particulate flow | 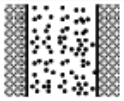 | Solid particles in gas or liquid | Transportation of powder |

Figure 2.3. Classification of two-phase flow (Source: Ishii & Hibiki, 2011)

In two-phase flows, the bubbles have little interaction at very low gas flows, but they increase in number and density as the gas flow rate increases, while distorted-spherical and discrete bubbles act in a simultaneous liquid phase of bubbly flow. The slug flow generally consists of small bubbles, which are bullet-shaped bubbles, also known as Taylor bubbles. A thin liquid film separates these bubbles from the wall. As a result of higher flow rates, bullet-shaped bubbles are subjected to splitting and disruption. Then, the slug flow is converted into churn flow by the disorganized motion.

With increasing gas flow rates, churn flow is converted into the annular dispersed flow. The bubbles then turn into droplets and the bubble diameter decreases to 10 – 100 μm. Another annular type flow is the inverted-annular flow that is not observed in adiabatic gas-liquid flows. Inverted-annular flow occurs where the wall has a high heat flux (Ghiaasiaan, 2008).

As mentioned before, the two-phase flow distribution is influenced by mechanical impurities, especially by geometrical factors. As shown in Figure 2.4, geometrical factors play a critical role in operating conditions.

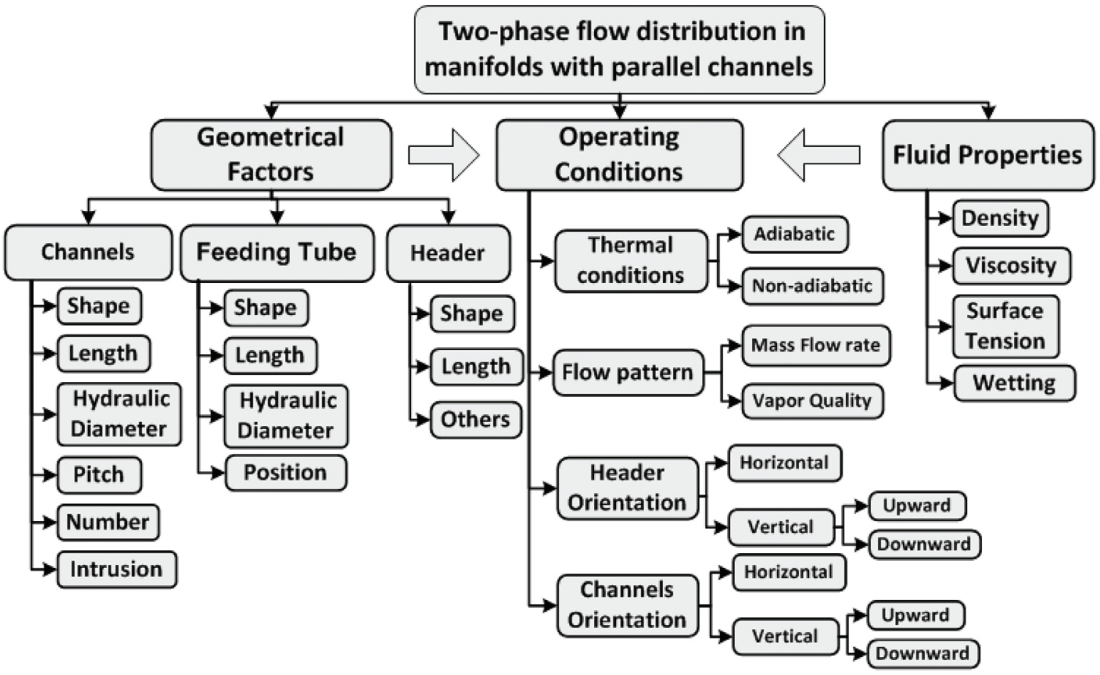


Figure 2.4. Factors influencing the two-phase flow distribution in headers with parallel channels (Source: Dario , Tadrist, & Passos, 2013)

Any changes in geometrical parameters (shapes or diameters) significantly influence flow structure. The operating conditions are not only affected by the geometrical factors but also influenced by fluid properties. However, the microchannel heat exchangers are usually used in close systems so that the fluid properties could be changed only with external factors. Factors, such as density, viscosity, are considered as operational conditions. Heat flux and change in flow regime are also included in operating conditions.

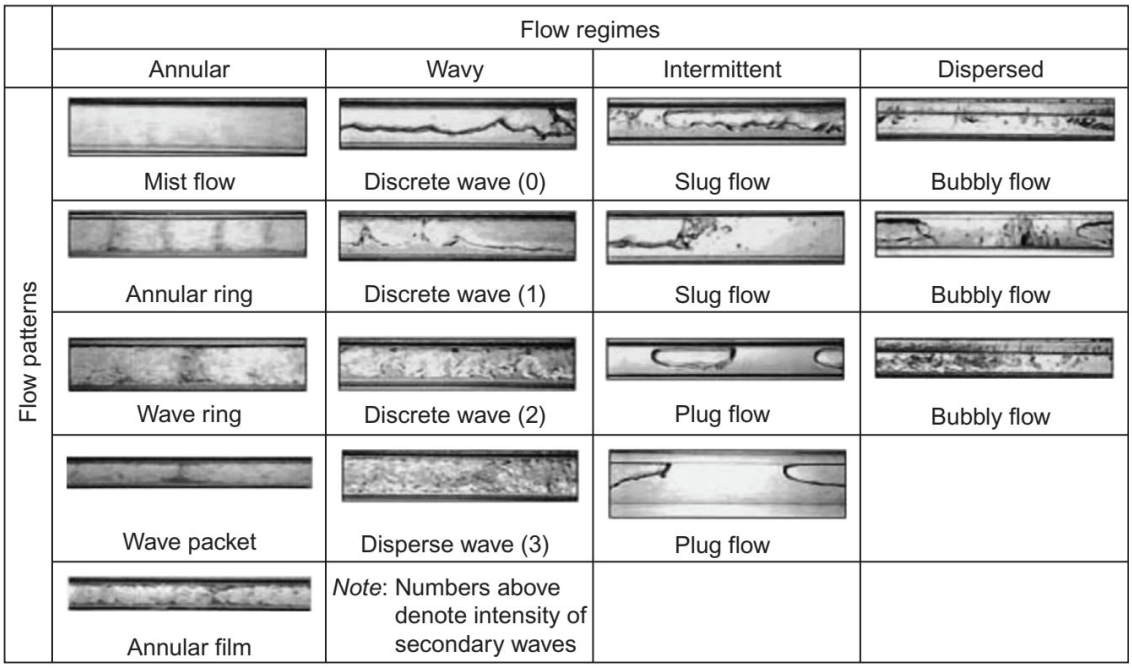


Figure 2.5. Condensation flow regimes and patterns (1 < D < 4.9 mm) (Source: Kandlikar, Garimella, Li, Colin, & King, 2006)

Condensation in the microchannel is more significant than before for increasing the efficiency of HVAC systems, power generators and chemical processes (Kandlikar, Garimella, Li, Colin, & King, 2006). The improvement of this field reduces the costs of using more compact microchannel heat exchangers. The development of chemical industries for new refrigerants also reduces harmful gases released into the environment (R-404a, R-410a).

## 2.2.2 Header Shapes, Inlet Direction and Protrusion

The header shapes with significant effects on flow distribution have been searched by different researchers for years. In one of the earliest studies, the inlet direction of fluid was studied using relevant equations (Bajura & Jones, 1976). The experimental study has also been performed with a different manifold profile. Wang, Yang, Tsai, & Chen (2011a) studied the factors affecting the flow distribution and reported that flow distributions were significantly influenced by flow area ratio, flow direction, inlet velocity, flow resistance, and gravity. The study described the flow direction as affected by the location of inlet and outlet flows from the manifold. In

Figure 2.6, more detailed effects of flow direction on flow distribution were described by (Webb & Chung, 2005). Different inlet and outlet locations, horizontal or vertical heat exchanger placements were experimentally studied.

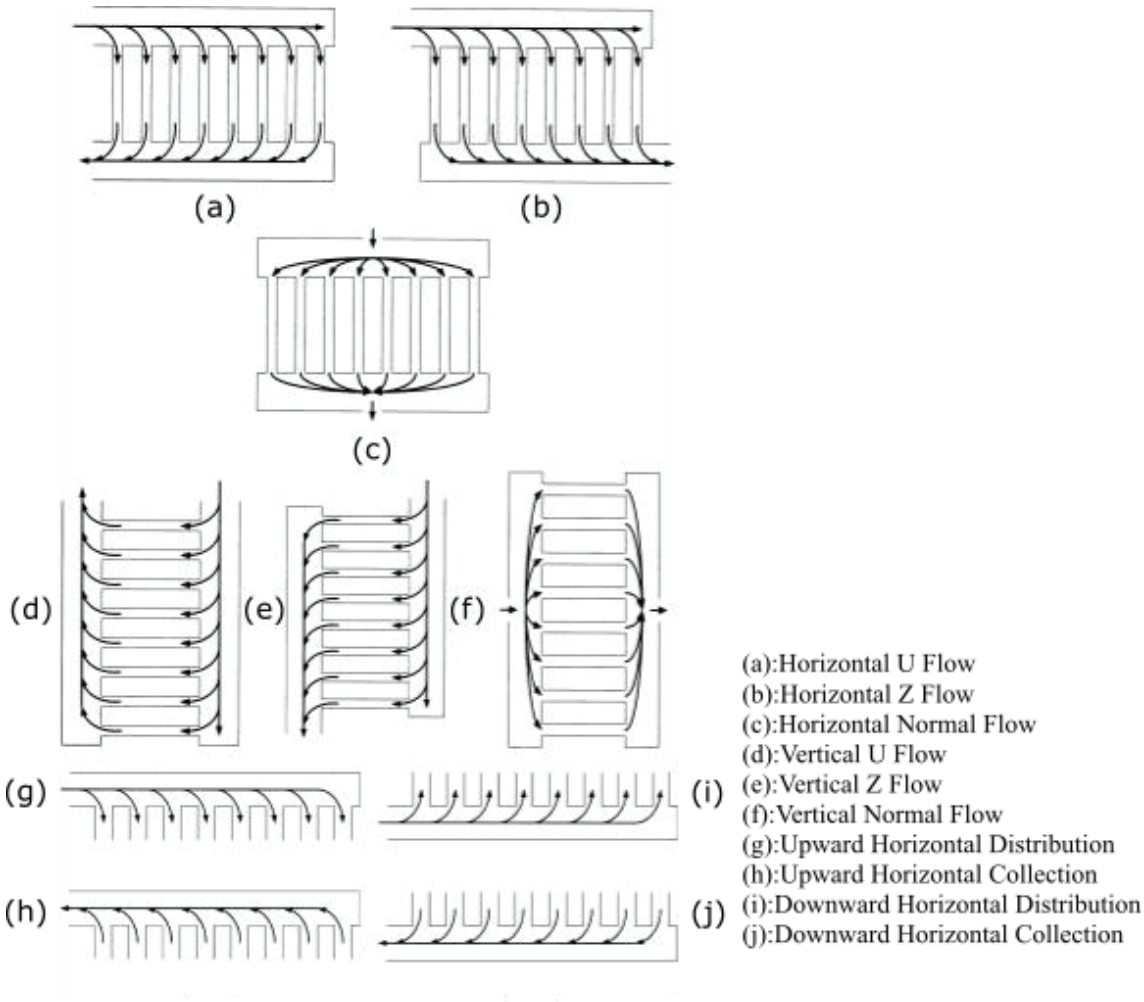


Figure 2.6. Manifold Types, Flow Directions in Manifolds and Channels Source: (Webb & Chung, 2005)

Inlet flow conditions also significantly influence the flow regimes of the heat exchangers. Ahmad, Berthoud, & Mercier, (2009) experimentally studied the loop representing a compact plate heat exchanger. A cylindrical horizontal header and eight rectangular channels were visualized in the header. Decreasing inlet diameters are more adaptive to two-phase flows. Also, expansion devices highly influence the flow structure to reach a homogenous flow distribution. Panghat & Mehendale, (2016) also studied the effects of upward/downward headers on two-phase flow. Just because of

gravity, the downward flow liquid ratio was higher than the gas flow ratio in the initial channels, so it was seen that gravity profoundly affected two-phase flow distribution.

On the other hand, there are many studies conducted with changing header shapes to reach a more homogenous flow distribution. The first inspiration for changing header shape is changing header diameter Cetkin, Lorente, & Bejan, (2010). Tuo & Hrnjak, (2013) studied different header diameters between inlet and outlet manifolds. Also, vertical and horizontal placement was investigated under different diameters of manifolds. Enlarging header sizes of the outlet significantly reduced the maldistribution effect. Many different approaches were numerically and experimentally studies (Tong , Sparrow , & Abraham , 2009). Researchers changed header shapes with taper angle, concave-down, and concave-up contoured type in upward distribution manifold. It was observed that geometrical construction enlarging the manifold area was better than the others. Therefore, concave-down and most straight-forward tapered shape yielded more reliable results for flow distribution. Minqiang, Dehuai, Yong, & Dongqing, (2009) investigated multi parallel microchannels with the triangle manifold numerically by CFD and indicated that symmetric manifold structure provided a more uniform velocity distribution. Cetkin, (2017) introduced a theoretical approach for header design and applied Tree-branching, Leonardo da Vinci and Hess-Murray Rules to manifold shapes to get uniform flow rate and distribution. As it was stated in constructal theory, the flow domain should be dynamic, so the new design was created iteratively based on the constructal law. It was observed that constructal design provided better flow distribution than the other designs and this uniformity was valid not only for pressure drop but also within the velocity profile.

Although the geometrical design was the primary issue for better flow distribution, another component of heat exchangers can also regulate the flow distribution. For instance, Wang, Yang, Tsai, & Chen, (2011b) modified the header by installing a baffle tube. Baffle tube holes had different diameters and locations. Flow distribution was less uniform in the initial channel than the rear channel, so flow continued to the end of the header but not uniformly as expected. To gain a uniform flow distribution, Shi, Qu, Qi, & Chen, (2011) designed a deflector, which is a plate with holes at different locations. The flow entered from the manifold and separated by the deflector holes. Seven different deflectors were designed to make the flow more uniform. The study was executed experimentally and adding deflectors into the inlet and outlet manifold significantly influenced flow distribution, but microchannel cost

increased more than it would be affordable. As can be seen, many approaches were availed to reach a more uniform flow distribution under entire operational conditions. The changes in design geometry generally had greater effects on homogeneous flow distribution than the new unit designs. Although new unit designs for manifold influenced flow regime, such designs significantly increased the costs of microchannel heat exchangers.

Besides changing manifold geometric shapes, the interaction between the manifold and the channel can also be changed. This more effective method, so-called protrusion or bulge, was mentioned in earlier studies. Marchitto, Fossa, Guglielmini, & Paietta, (2014) investigated phase distribution in a parallel upward heat exchanger. The channels were inserted into the header with different configurations. The phase separation and uniform flow distribution were expected. The attained data showed that if the dimensionless depth was higher than 0.5, then the phase distribution was affected positively. Even at the higher liquid velocity, protrusion of the channel yielded more uniform flow distribution with the highest protrusion depth. Koyama, Wijayanta, Kuwahara, & Ikuta, (2006) studied refrigerant flow with three different header configurations. The header configurations were adjusted with the embedded channels. The embedding ratio was half diameter of the header. It was reported that refrigerant liquid was distributed easily and better distribution of the vapor phase was achieved. Such interactions between the channel and the header yielded more reliable, cheaper and feasible outcomes. Therefore, the new header design may be a kind of technique to achieve a more uniform flow distribution.

# CHAPTER 3

# NUMERICAL MODEL & METHOD

## 3.1 Numerical Model

Within the scope of computational fluid dynamic (CFD), initially, numerical researches and studies have been conducted. Particularly, the new design theory offers more effective use of CFD software since the software yields quite close results to experimental values. However, such software requires powerful computers, not special sensors, valves or thermocouples and other devices. With the developments achieved in CFD software, researchers can create more proper designs.

Pressure drops, heat transfer rates, design mass-flow rates and fluid dynamic forces, such as lift and drag, can all be calculated using CFD. It employs the finite element method, a discretization technique used in structural and thermal analysis. The subdivision of the mathematical model into non-overlapping components of simple geometry called finite elements is the fundamental concept in the physical interpretation of the FEM.

The reference geometry is presented in Figure 3.1. The reference geometry has eight channels with a rectangular header. The channels have 0.01 cm baffle thickness between each other. Total heat exchanger size is 4.00 cm x 4.07 cm, including header diameter and the baffle thickness. The baffle thickness was chosen by adding 0,7 cm to the height of heat exchanger involved in baffle thickness. In the reference study, header diameter was expressed as D, an abbreviation of diameter. This study used two different ratios, area ratio and width ratio. The area ratio is defined as the ratio of total channel cross-section area to header cross-section area, while the width ratio is defined as the ratio of combined header cross-section area to header cross-section area. Firstly, area ratio was chosen as 16. Therefore, D was calculated using other geometrical measurements as 0.25 cm. Also, w is the channel width, and it was measured as 5 cm for each channel.

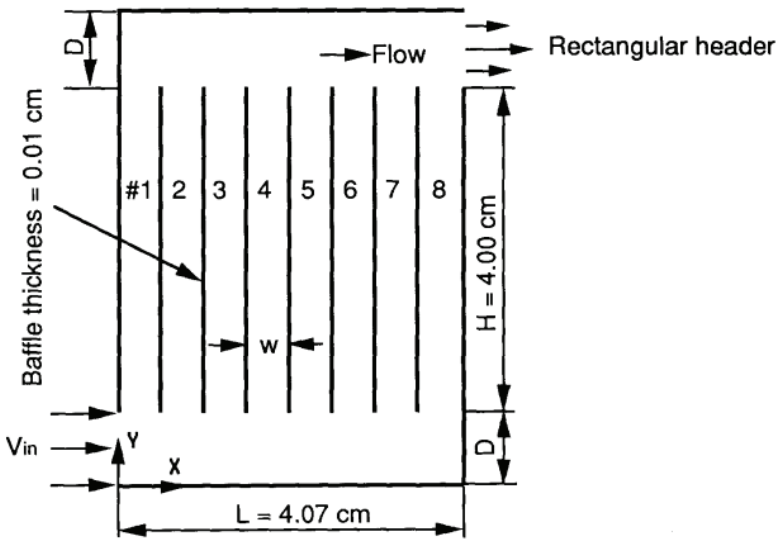


Figure 3.1. Reference Geometry (Source: Kim, Eunsoo Choi, & Young I. Cho, 1995)

The geometry was modeled with the SOLIDWORKS option of CAD software. Then, the model was imported into SpaceClaim platform of ANSYS CAD program. The model was a 2D model and interfaces were defined as surface. ANSYS Workbench Mesher software was used for mesh generation of the model. The elements were quadratic and the growth rate of mesh was defined as 1,05 to achieve a more suitable mesh at the corners of the geometry. The inflation of mesh was opened and transition ratio was set as 0.272.

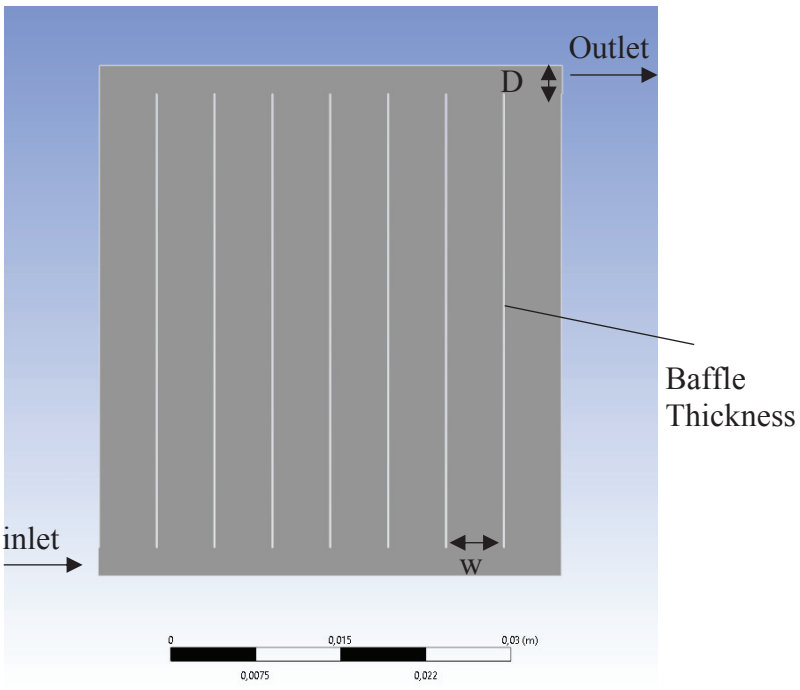


Figure 3.2. Modelled Geometry

## 3.2 Governing Equations

Laminar incompressible flow equation of (Silva, Lorente, & Bejan, 2004) was used for present microchannel heat exchanger model. The assumption was Newtonian fluid for two-dimensional geometry. The flow was steady state and governed by the continuity and Navier-Stokes's equations. In the most basic form, the dimensionless equation is defined as follows;

$$\frac{\partial u}{\partial x} + \frac{\partial v}{\partial y} = 0 \tag{3.1}$$

$$\rho(u\frac{\partial u}{\partial x} + v\frac{\partial u}{\partial y}) = -\frac{\partial p}{\partial x} + \frac{1}{\mu}(\frac{\partial^2 u}{\partial x^2} + \frac{\partial^2 u}{\partial y^2}) \tag{3.2}$$

$$\rho(u\frac{\partial v}{\partial x} + v\frac{\partial v}{\partial y}) = -\frac{\partial p}{\partial y} + \frac{1}{\mu}(\frac{\partial^2 v}{\partial x^2} + \frac{\partial^2 v}{\partial y^2}) \tag{3.3}$$

The VOF (Volume of Fluid) model is a surface-tracking model for two or more immiscible fluids where the position of the interface between the fluids is of interest. The solution of a continuity equation for the volume fraction of one (or more) of the phases is used to track the interface(s) between the phases. The computational cell is tracked throughout the domain while a single set of momentum equations is shared by the fluids. For instance, this model is used for filling and emptying of the tanks.

The mixture model can model two-phase flows with only two main equations, momentum and continuity equations for the mixture. An algebraic expression is used for the relative velocity and the volume fraction is also modeled for the secondary phase.

The Eulerian model is the most complex model. It solves a set of n momentum and interpenetrating continua equations. Fluidized bed, mixture of immiscible fluids, is also included in the application.

$$\frac{\partial}{\partial t}(\alpha_q \rho_q) + \nabla.(\alpha_q \rho_q \vec{v}_q) = \sum_{p=1}^{n}(\dot{m}_{pq} - \dot{m}_{qp}) + S_q \quad (3.6)$$

Here $\vec{v}_q$ is the velocity of phase q and $\dot{m}_{pq}$ characterizes the mass transfer from every phase of p and q same with $\dot{m}_{qp}$ term. These mechanisms can customize separately. $S_q$ is the source term.

Volume fractions represent the space occupied by each phase, and each process independently satisfies the laws of mass and momentum conservation. Therefore, the volume of phase q,$V_q$ is defined by;

$$V_q = \int_V \alpha_q \, dV \quad (3.7)$$

where;

$$\sum_{q=1}^{n} \alpha_q = 1 \quad (3.8)$$

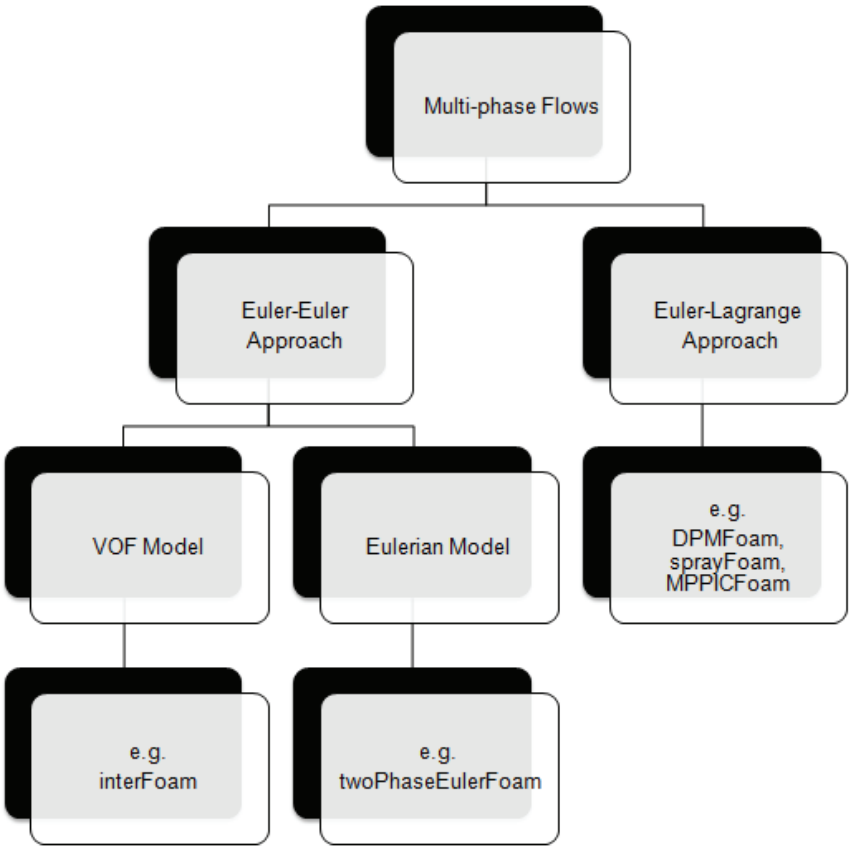


Figure 3.3. Steps for modelling methodology for multi-phase flow (Source: Multi-Phase Flows And Discrete Phase Modelled, 2020)

The Lee model is a physical-based model. The model is used with the mixture and VOF multiphase models as well as with the Eulerian multiphase model if one of the overall interfacial heat transfer coefficient models were used. The liquid-vapor mass transfer (evaporation and condensation) is governed by the vapor transport equation in this model.

$$\frac{\partial}{\partial t}(\alpha_v \rho_v) + \nabla.(\alpha_v \rho_v \vec{V_v}) = \dot{m}_{lv} - \dot{m}_{vl} \tag{3.4}$$

Where; v is the vapor phase, $\alpha_v$ is the vapor volume, $\rho_v$ is the vapor density (kg/m$^3$), $\vec{V_v}$ is the vapor phase velocity (m/s) and $\dot{m}_{lv}, \dot{m}_{vl}$ = the rates of mass transfer due to evaporation and condensation (kg/s).

If $T_l > T_{sat}(Evoparation), then$

$$\dot{m}_{lv} = coeff \times \alpha_l \rho_l \frac{(T_l - T_{sat})}{T_{sat}} \tag{3.5}$$

If $T_v < T_{sat}(Condensation)$, then

$$\dot{m}_{vl} = coeff \times \alpha_v \rho_v \frac{(T_{sat} - T_v)}{T_{sat}} \tag{3.6}$$

Where; coeff designates a coefficient. It can be interpreted as a relaxation time. The $\alpha$ is the phase volume fraction and ρ is the density.

The thermal phase change model was used when the Eulerian multiphase model was used.

For liquid phase from the interface;

$$Q_l = h_l A_i (T_s - T_l) - \dot{m}_{lv} H_{ls} \tag{3.7}$$

For vapor phase from the interface;

$$Q_v = h_v A_i (T_s - T_v) - \dot{m}_{lv} H_{vs} \tag{3.8}$$

Where; $h_v$ and $h_l$ are vapor and liquid phase heat transfer coefficients, respectively. $H_{ls}$ and $H_{vs}$ are the liquid and vapor enthalpies. $T_s$ is the surface tension. If $T_s = T_{sat}$ is neglected (sat designating saturation), then, surface tension temperature could be equal to saturation temperature.

The energy that changes the temperature of the material without causing phase change is known as sensible heat although absorbed or released by a material during a phase change from a gas to a liquid or a solid is known as latent heat. The equations of sensible and latent enthalpies are while the phase is changing;

$$h = h_l + h_g$$
$$\text{where } h_g = \int_{T_{ref}}^{T} C_p \, dT \text{ and } h_l = fL \tag{3.8}$$

$$h = \begin{cases} \int_{T_{ref}}^{T_{gaseous}} C_p \, dT & if \; T < T_{gaseous} \\ \int_{T_{liquidus}}^{T_{gaseous}} C_p \, dT + fL & if \; T_{liquidus} < T < T_{gaseous} \\ \int_{T_{liquidus}}^{T} C_p \, dT & if \; T_{liquidus} < T \end{cases} \tag{3.9}$$

The amounts of heat transmitted through a surface are referred to as a heat flux or thermal flux. The equation

$$\dot{q} = \dot{Q}/A \tag{3.7}$$

Here $\dot{q}$ is heat flux, $\dot{Q}$ is heat and $A$ is the total surface area.

## 3.3 Validation and Mesh Independency

The meshed geometry simulated a pressure-based steady state. The gravity forces were loaded in the -y-direction. The viscous model was chosen as laminar. The flow Reynold's number was given in the references as 50, 100, 200, and 300, but the

analytically validated Reynolds number is 50, so Reynold's number was chosen 50. The fluid is water and the viscosity and density of water are constant, respectively as $\mu$=0,01002 g/cm.s and $\rho$=0,9982 g/cm$^3$ at 20°C.

The mesh size was decreased until the criteria of $10^{-3}$ were satisfied. Relative numerical errors corresponding to the mesh size can be seen in Table 3.1 Solution became mesh-independent with 180 400 elements by the relative errors reaching in channel 5 to $1{,}75.10^{-3}$.

Table 3.1. Relative errors corresponding to the number of mesh elements

| Mesh Independency | | Average Velocity Values for Channels | | Relative Errors | |
|---|---|---|---|---|---|
| | | Average Velocity Channel #4 | Average Velocity Channel #5 | Average Velocity Channel #4 | Average Velocity Channel #5 |
| 1 | 14605 | 1,97E-03 | 1,71E-03 | --- | --- |
| 2 | 29084 | 4,15E-04 | 3,33E-04 | 1,56E-01 | 1,38E-01 |
| 3 | 80367 | 1,97E-03 | 1,59E-03 | 1,56E-01 | 1,26E-01 |
| 4 | 180400 | 1,84E-03 | 1,57E-03 | 1,30E-02 | 1,75E-03 |

In Figure 3.4, the current study was validated with the (Kim, Eunsoo Choi, & Young I. Cho, 1995) with almost exact match of flow ratio. The figure also shows the flow ratio percentage in each channel.

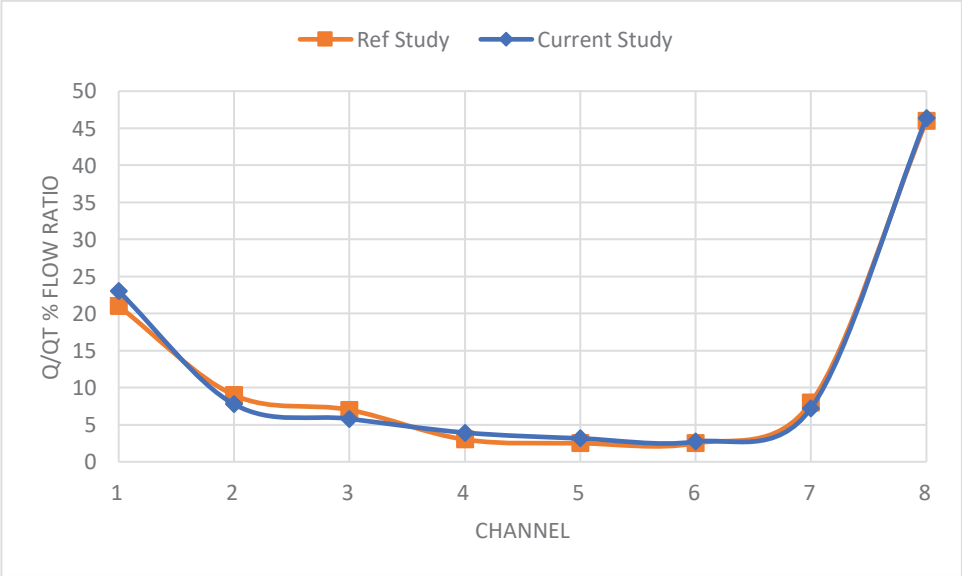


Figure 3.4. The result comparison the current study with (Kim, Eunsoo Choi, & Young I. Cho, 1995)

## 3.4 Materials

The fluid properties are also notable features for all cycles. For condensers, refrigerant fluids are used in the cooling cycle. A refrigerant fluid in a refrigeration device works as a heat sink at low temperatures and dissipates the heat at higher temperatures. Moving the heat from a lower to a higher temperature necessitates refrigerant operation (Jobson, 2014).

In the referenced study, water was used as a coolant fluid. However, to expect higher performance from the condenser, refrigerant fluids should be used in the cycle. Technically, remarkable refrigerant fluids have to low freezing point, low condensing pressure, and high evaporator pressure with an affordable price and low toxicity. Therefore, R410a is a nearly azeotropic combination of R-125 and R-32 that is now mainly used in modern air conditioners. R410a has higher refrigerating performance and much higher pressures than other refrigerants. Since this mixture is not azeotrope, it must always be moved and loaded in the liquid phase. It is a chemically stable substance with low toxicity and low-temperature glide (Gas Servei Technical Data Sheet).

Standard state enthalpy is one of the properties; vapor and liquid phase are set such that their difference equals the latent heat of vaporization. The calculation technic of standard state enthalpy is simple. Latent heat value kJ/kg multiply with the molecular weight. In this case;

$$H(T_{ref}) = 2.2059E7 \text{ j/kmol}$$

All other properties of R410a are given in Table 3.2 Each equation is written by piecewise polynomial at the range of temperature in the specified gap for equations except heat capacities values. These values are written polynomial in the gap because the temperature ranges are not given at the working range.

Table 3.2 The R410a thermodynamic properties by the equations for property estimation at Reference Temperature 233.15K (Source: Freon, 2019)

| Liquid Phase |
|---|
| Saturated Liquid Viscocity (kg/m.s) (223.15K to 343.15K)<br>$\mu = 166E\text{-}04 - 2.25E\text{-}06\ T + 1.81E\text{-}8\ T^2 - 9.20E\text{-}11\ T^3$ |
| Liquid Saturated Heat Capacity J/kg K (233.15K to 323.15K)<br>$Cp = 1.603E\text{-}3 + 5.727E\text{-}6\ T + 9.903E\text{-}8\ T^2 + 1.855E\text{-}9\ T^3$ |
| Saturated Thermal Conductivity in (W/m-K) (253.15K to 343.15K)<br>$k = 1.001E\text{-}1 - 4.71E\text{-}4\ T + 6.86E\text{-}7\ T^2 - 1.29E\text{-}8\ T^3$ |
| Vapor Phase |
| Gas Viscocity At Atmospheric Pressure (kg/ms) (243.15K to 393.15K)<br>$\mu = 1.170E\text{-}2 + 3.98E\text{-}5\ T$ |
| Ideal Gas Heat Capacities (J/kgK) at constant volume<br>$Cv = 2.63E\text{-}4 + 2.12E\text{-}6\ T - 9.85E\text{-}10\ T^2 + 6.49E\text{-}14\ T^3$ |
| Vapor Thermal Conductivity at Atmospheric Pressure (W/m-K)<br>$k = 1.154E\text{-}2 + 7.41E\text{-}5\ T$ |
| Other Properties |
| Molecular Weight<br>72.58 |
| Boiling Temperature at Atmospheric Pressure<br>221.57 K |
| Latent Heat of Vaporization ( at 1.013 bar)<br>276 kJ/kg |

## 3.5 Boundary Conditions

With the assignment of the governing equations and identified material properties, initial and boundary conditions are defined practically working refrigerant cycle by the integrated geometrical improvements design at the end of the study.

For that, there should be a specified model setup. In this case, the multiphase function was expressed which was define governing equation. The energy equation was valid and viscous equations are set up laminar. On the laminar setup option, viscous heating was opened. All those settings define the governing equations that on valid for the model.

Boundary conditions settings were identified by name of the inlet, outlet, fluid (interior fluid) and wall. Inlet and outlet were chosen velocity-inlet and outflow, respectively.

The solution methods scheme was chosen Phase-Coupling SIMPLE. On this selection, there was an option; it is the N-Phase volume fraction equations. The phasic momentum and volume fraction equations, significantly coupled with the shared pressure in multiphase flow. Commonly, some variation of the SIMPLE algorithm is coupled with the shared pressure with the momentum equations by the advance of transforming the total continuity into a shared pressure; the Fluent software Phase Coupled SIMPLE algorithm has been successfully performed and determines a wide range of multiphase flows. However, some of the problems occur by the non-symmetric resulting matrix and the continuity constraint may contribute to a zero-diagonal block, which makes it difficult to find a result. To avoid these types of problems, Fluent reconstructs a pressure correction equation (Fluent User's Guide, 2013).

$$\begin{pmatrix} A_p & C_{U1} & C_{U2} & D_{\alpha 2} \\ B_{U1} & A_{U1} & A_{U12} & D_{U2} \\ B_{U2} & A_{U21} & A_{U2} & D_{U2} \\ E_p & E_{U1} & E_{U2} & A_{\alpha 2} \end{pmatrix} \begin{pmatrix} \acute{p} \\ \acute{U}1 \\ \acute{U}2 \\ \acute{\alpha}2 \end{pmatrix} = \begin{pmatrix} S_p \\ S_{U1} \\ S_{U2} \\ S_{\alpha 2} \end{pmatrix} \tag{3.9}$$

Phasic velocity correction components are $\acute{u_k}, \acute{v_k}$ and $\acute{w_k}$ where the k present phase notation $\acute{p_k}$ and $\acute{\alpha_k}$ are the shared pressure correction and volume fraction correction, respectively. Therefore, equation (3.9) can be easily generalized to n phases.

# CHAPTER 4

# NUMERICAL RESULTS & DISCUSSION

## 4.1 Minichannel Heat Exchanger

In present heat exchanger, channel width was the primary classification parameter as it is mentioned before. Figure 4.1 below shows the velocity and the static pressure distribution in a rectangular header and presents the results of reference geometry. Given the velocity profile, maldistribution can clearly be seen in Figure 4.1. The static pressure distribution of heat exchanger was higher near the inlet location and lower near the outlet location. Such a case was encountered due to the inverse proportion between velocity and pressure. Therefore, it was observed that the velocity profile influenced pressure profile.

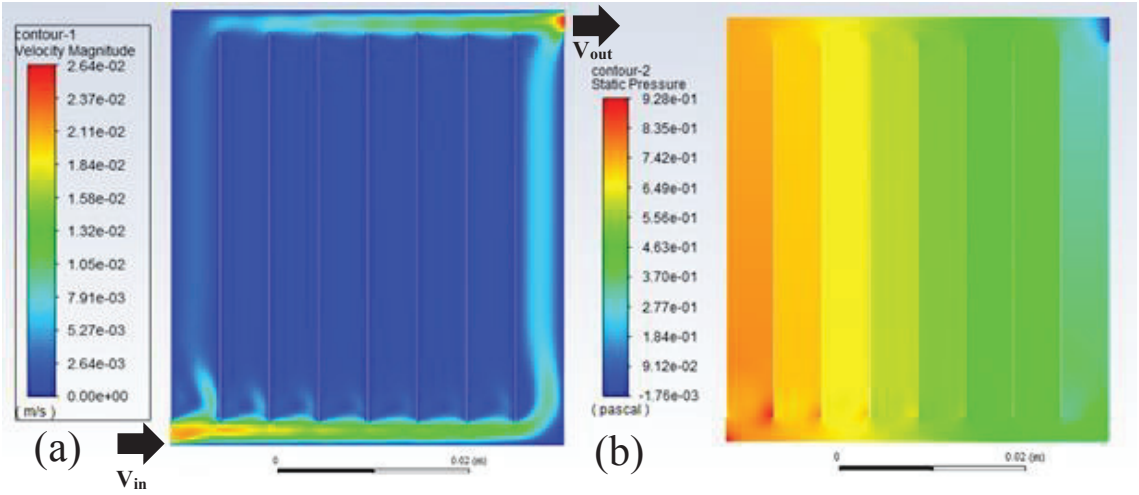


Figure 4.1. Minichannel (a) Velocity Profile (b) Static Pressure, Re=50

The parameters reported above were directly influenced by flow rate of the heat exchanger. Figure 4.2 below shows the volume flow rate for each channel in the heat exchanger. As shown in the figure, the first and the last channels had greater volume flow rates than the other channels. The irregularity of flow rate altered the heat exchanger performance.

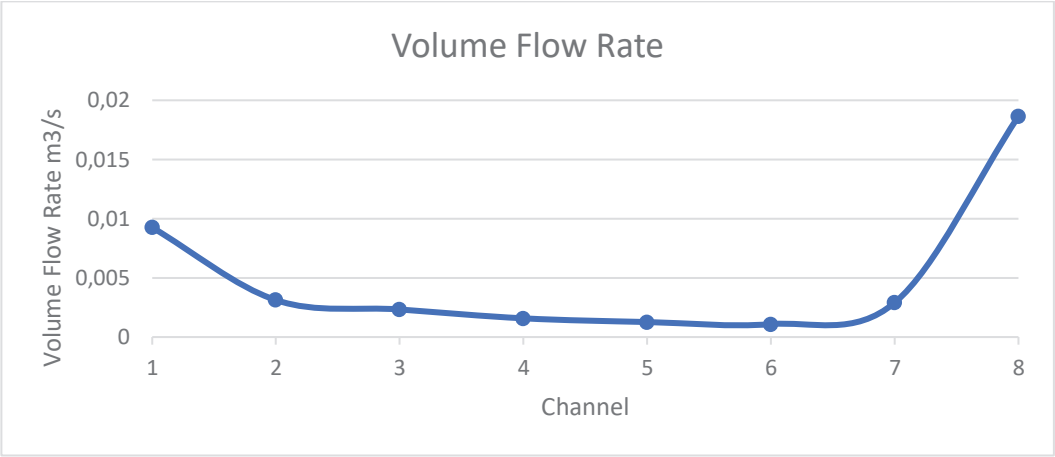


Figure 4.2. Minichannel volume flow rate, Re=50

Concerning thermal performance of the heat exchanger, it was observed that the configuration of heat exchange could be depicted via (Vist & Pettersen, 2004) study. The only difference from that study was the refrigerant fluid since water was the refrigerant fluid in present study. Both heat exchangers were used as condenser; thus, the inlet temperature was higher than the outlet temperature. The thermal configuration for the inlet temperature was performed at 40°C, 50°C and 60°C. To consider the geometrical difference, current study temperature was chosen as 35°C at the inlet. The wall temperature was selected constantly as 15°C. All of the configurations were applied to current domain; the temperature of heat exchange is showed in Figure 4.3. Expected maldistribution did not have significant effects on thermal performance of the heat exchanger.

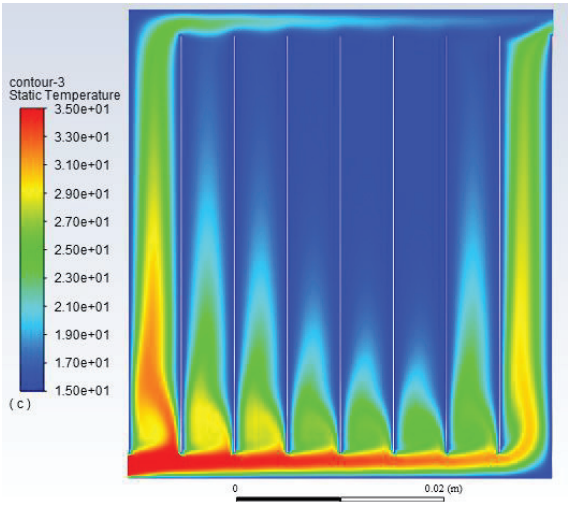


Figure 4.3. Minichannel thermal performance

## 4.2 Variety of Improvements in Heat Exchanger Design

With the effects of flow maldistribution, the heat exchanger performance was decreasing dramatically. The geometrical changes strongly influenced flow distribution (Mueller & Chiou, 1988). On this part, some of geometrical changes were applied to current study in this thesis to improve the heat exchanger performance.

### 4.2.1 Increasing the Thermal Performance

The thermal performance is relatively related to heat surface area. For the heat exchangers, channel dimensions should be minimized to increase the surface area. For that purpose, in current geometrical model, channels were doubled and the channel dimensions were reduced by 1.13 mm (Figure 4.4); thus, the heat exchanger had microchannels (Kandlikar & William J. Grande, 2003). All the other geometrical configurations were the same with the first domain.

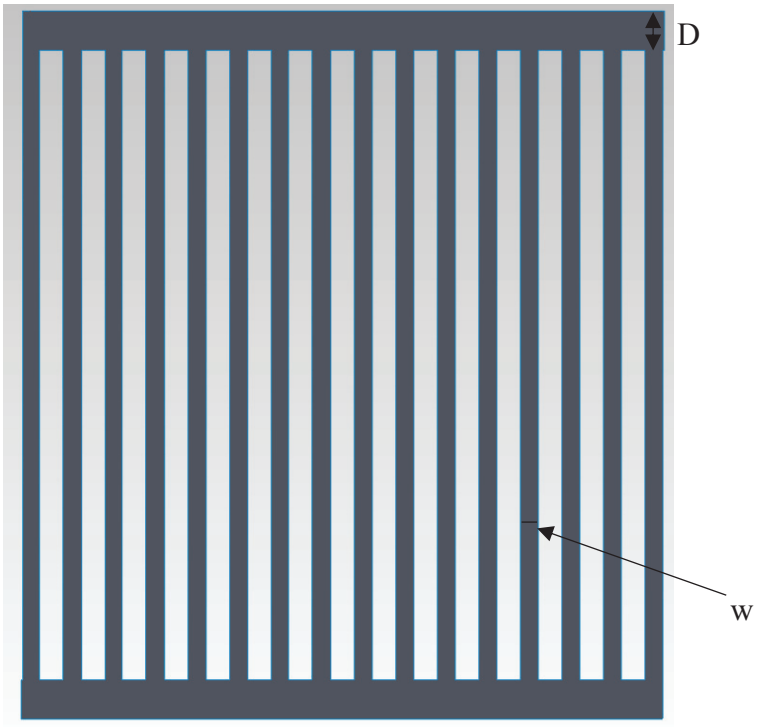


Figure 4.4. The improved design geometry

As shown in Figure 4.5, the thermal performance of heat exchanger was highly improved as compared to the first domain. The configuration of flow was almost identical with the first configuration; thus the Reynolds number was 50. Within the advance of thermal performance, the flow rate can be increased through raising the capacity of heat exchanger.

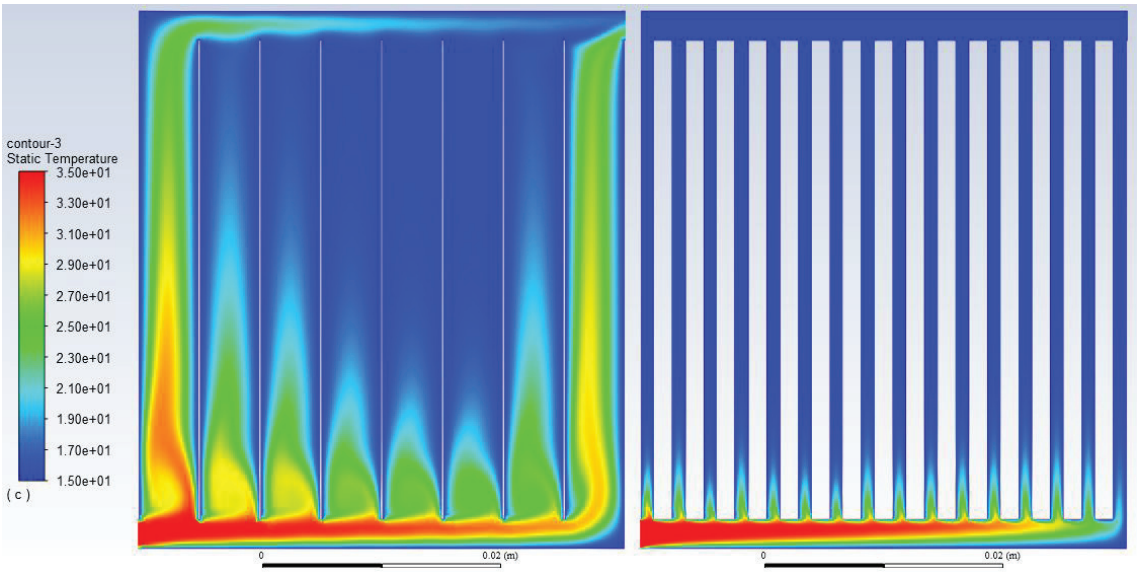


Figure 4.5. Impact of channels configuration for the thermal performance

On the other hand, the gravity significantly influences the fluid flow. Gravity changes flow characteristics when the direction of flow was opposite of the gravity. Therefore, the inlet and outlet can be switched to eliminate the gravity forces (Figure 4.6).

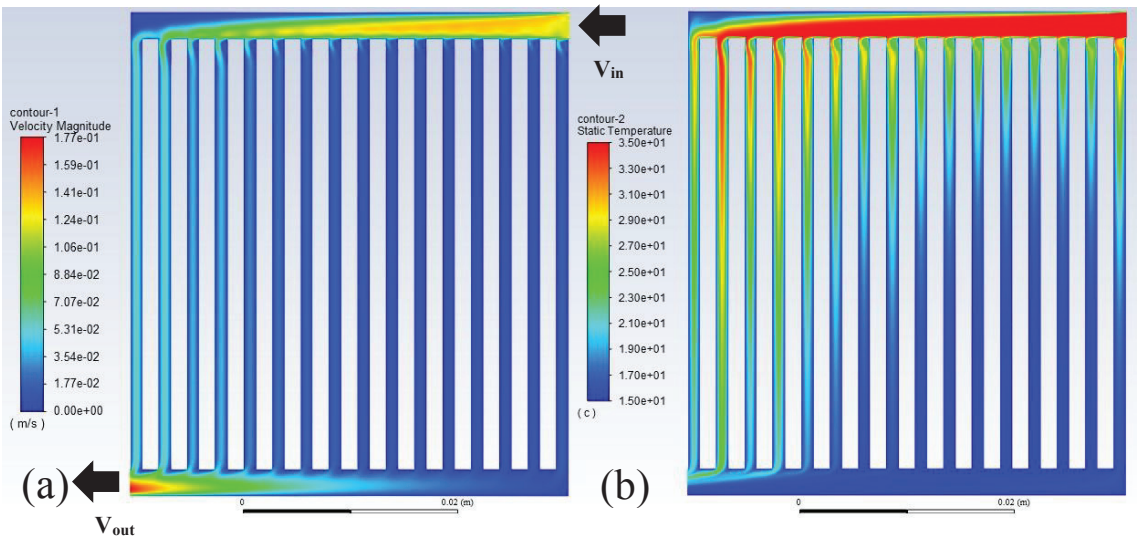


Figure 4.6. Improved design (a) Velocity profile (b) Static temperature distribution Profile, Re=300

As flow rate increases, effects of maldistribution on microchannel heat exchanger performance increases. Figure 4.7 shows the obvious effects of resultant maldistribution on the flow. Switching inlet and outlet resulted in increased flow rates in rear channels of the heat exchanger. The diversification of the flow rate influenced the thermal performance of heat exchanger. The rear channels had higher flow rates than the middle channels of heat exchanger. As a consequence of this effect, the heat exchanger performance decreased with the unutilized channels.

Figure 4.7 shows the local statis pressure of each channel. The localization was provided with a horizontal line dividing microchannels into halves. The pressure distribution fluctuated in the channels. A dramatic decrease was observed in pressure of 11 and 12$^{th}$ channels. On the other side of microchannel heat exchanger, channels had more stable pressure distribution. The nonuniform flow distribution effect can be seen with greater number of flow parameters.

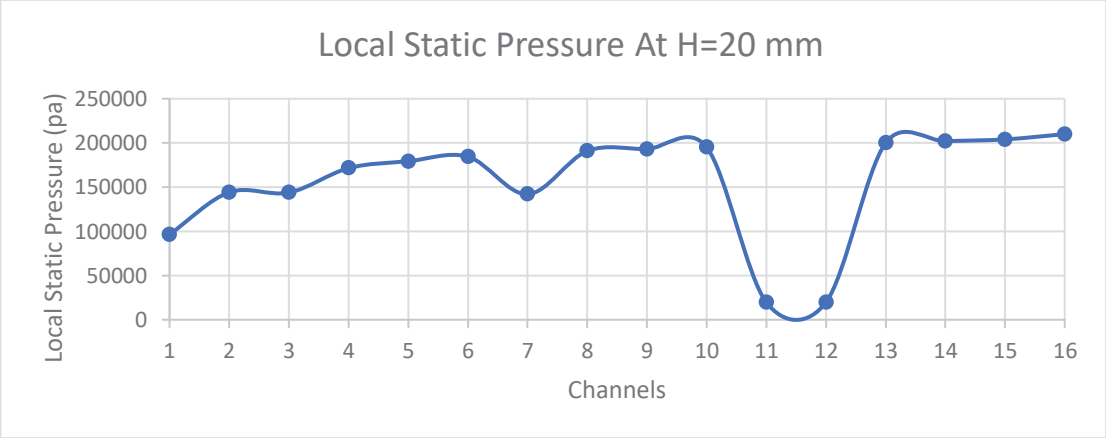


Figure 4.7. Local pressure distribution of the improved design

### 4.2.2 Enhancing Uniformity of Flow Distribution

The flow distribution is highly significant for the efficiency and performance of microchannel heat exchanger. With the improved maldistribution, the microchannel heat exchangers could have greater performance with the same dimensions or more compact microchannel heat exchangers could be designed. To achieve that, maldistribution effect should be reduced and the flow should be more uniform.

### 4.2.2.1 Effects of Header Shapes on Flow Distribution

As mentioned before, many researchers have tried to reduce maldistribution through changing some design parameters. The header shape and channel positioning are more effective approaches than the other approaches. Firstly, to enhancing flow distribution or to reduce maldistribution, the geometrical parameters were changed with the header shapes. Figure 4.8 shows the tapered header shape of microchannel heat exchanger. The channels were constant and the header dimension was the same. Comparison of different header shapes is presented in Figure 4.9.

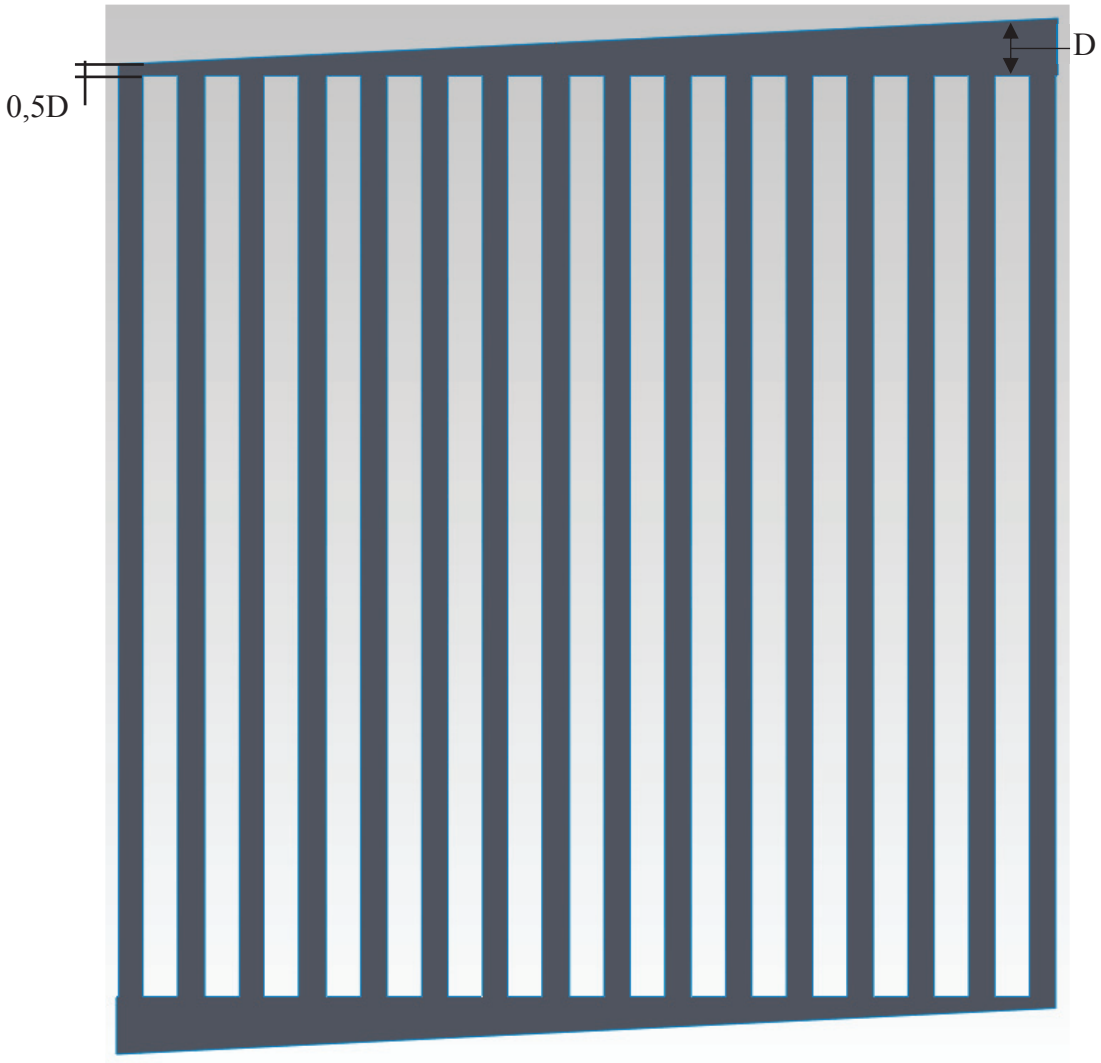


Figure 4.8. Enhancing uniformity with tapered header shape geometry

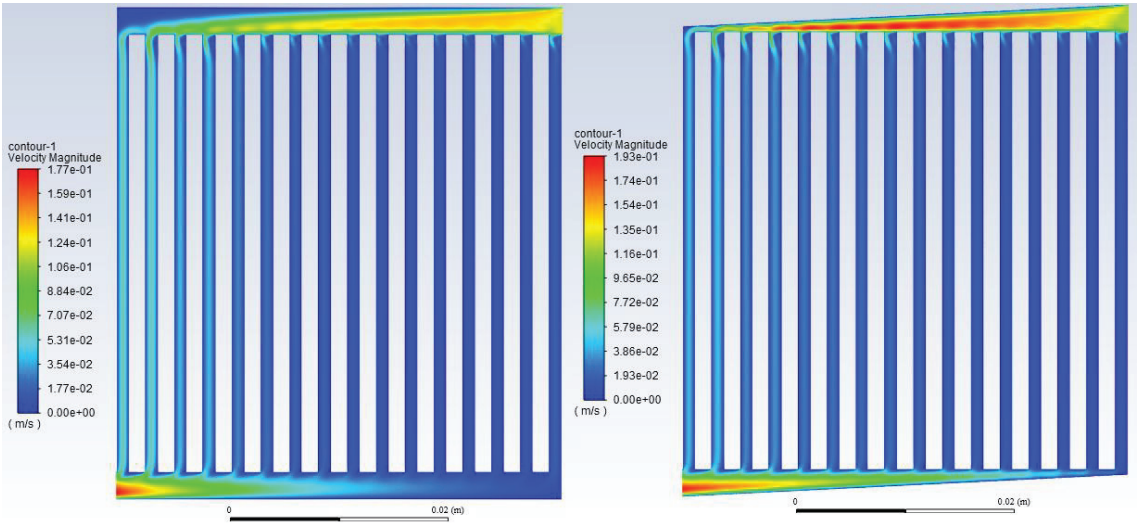


Figure 4.9. Comparison of header shapes

Concerning enhancement of header shapes, it was observed that the velocity profile was more stable in tapered headers as compared to regular form of the microchannel heat exchangers. The velocity magnitude of a channel was close to velocity of neighboring channel. As a result of the tapered header shape, middle channels had greater flow rates than the regular form of header. Furthermore, the flow rate values of regular microchannel and tapered microchannel are presented in Figure 4.10.

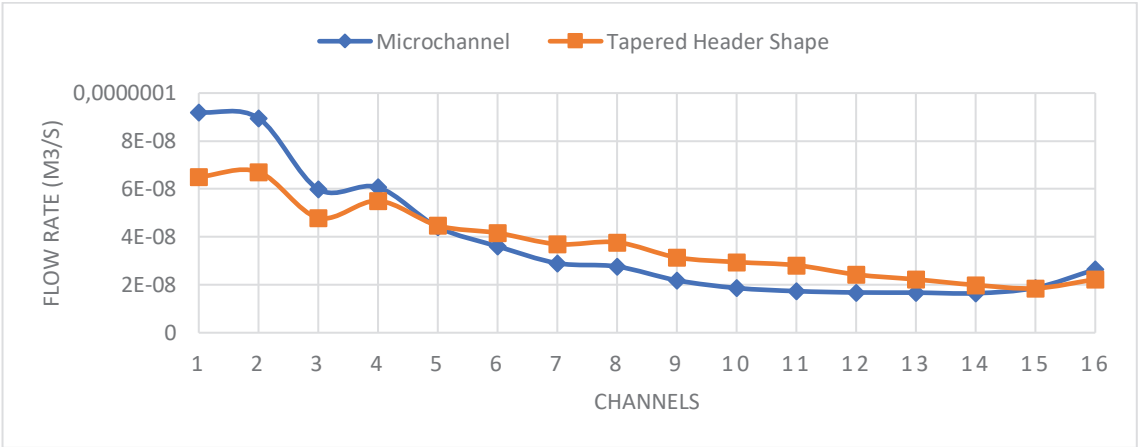


Figure 4.10. Flow rate regular and tapered header shape

When two header shapes were compared, it was observed that tapered header shape of microchannel heat exchanger slightly influenced the flow distribution. Flow rate of front channels decreased, thus, rear channels had more uniform flow distribution with the effects of tapered geometry.

To analyze the thermal effect, the static temperature distribution is presented in Figure 4.11. As an expected, improved flow distribution slightly influenced temperature distribution. The initial channels of microchannel had a low temperature distribution. Therefore, the efficiency of microchannel heat exchanger was slightly improved by changing header shapes.

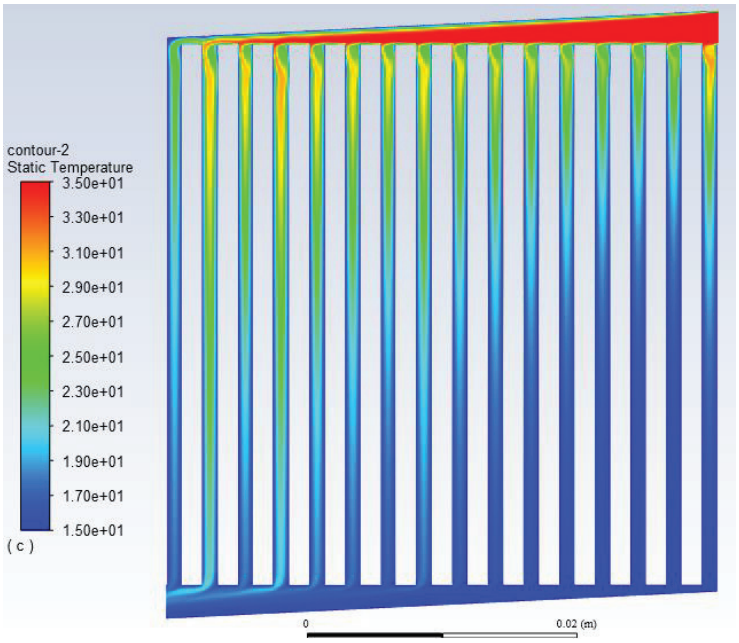


Figure 4.11. Static temperature distribution of tapered header shape microchannel

### 4.2.2.2 Effects of Channel Protrusion Depths on Flow Distribution

The capacity of heat exchangers is classified by the heat transfer ability. To increase that, protrusions are introduced into the geometry to increase the heat transfer surface and reduce the effects of maldistribution, then to improve the performance of heat exchanger. Thus, the tapered header shape of microchannel heat exchanger was analyzed since it was efficient in previous section. Here, the channel position in the header was considered (Figure 4.12).

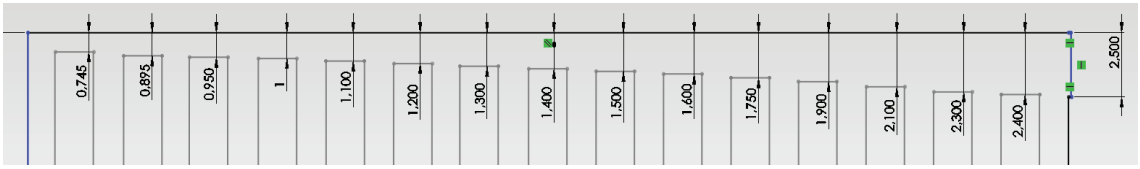


Figure 4.12. An example of channel positioning iteration configuration

Table 4.1 provides relative position of the channels to the bases point. The geometrical position of the channels and tapered shape had positive effects on flow distribution. Therefore, position of the rear channels was kept close to the border of inlet header top point. From the first iteration, every iteration was analyzed with applying the same procedure of references using Ansys Fluent software. The mesh independency test was also conducted and relative error value was lower than $10^{-3}$ when 93 400 elements were generated. The flow properties and assumptions were set the same in the solver software fluent within the evolution of geometrical improvement design settings. The refrigerant fluid was liquid water, the fluid flow was laminar and the energy equations were on. The Reynolds number was chosen as 300 for each iteration.

Here in Table 4.1, iterations were listed with the positioning of each wall height between channels and the top of header. At the end of iterations, flow rate value was collected from the solver software for each iteration.

Table 4.1. Channel positioning dimension for every iteration

| Height | Wall Height between Channels from the Top of Header | | | | | | | | | | | | | | |
|---|---|---|---|---|---|---|---|---|---|---|---|---|---|---|---|
| **2,5** | **1** | **2** | **3** | **4** | **5** | **6** | **7** | **8** | **9** | **10** | **11** | **12** | **13** | **14** | **15** |
| Iteration 1 | 2.5 | 2.35 | 2.2 | 2.05 | 1.9 | 1.75 | 1.6 | 1.45 | 1.3 | 1.2 | 1.1 | 1 | 0.9 | 0.8 | 0.65 |
| Iteration 2 | 2.4 | 2.3 | 2.1 | 1.9 | 1.75 | 1.6 | 1.5 | 1.4 | 1.3 | 1.2 | 1.1 | 1 | 0.95 | 0.895 | 0.745 |
| Iteration 3 | 2.35 | 2.3 | 2.1 | 1.9 | 1.75 | 1.6 | 1.5 | 1.4 | 1.3 | 1.2 | 1.15 | 1.1 | 1 | 0.95 | 0.6 |
| Iteration 4 | 2.4 | 2.35 | 2.1 | 1.9 | 1.75 | 1.6 | 1.5 | 1.4 | 1.3 | 1.2 | 1.1 | 1.05 | 1 | 0.9 | 0.65 |
| Iteration 5 | 2.4 | 2.375 | 2.1 | 1.9 | 1.75 | 1.6 | 1.5 | 1.4 | 1.3 | 1.2 | 1.1 | 1.1 | 1 | 0.8 | 0.75 |
| Iteration 6 | 2.35 | 2.325 | 2.1 | 1.9 | 1.75 | 1.6 | 1.5 | 1.4 | 1.3 | 1.2 | 1.1 | 1 | 0.9 | 0.8 | 0.7 |
| Iteration 7 | 2.4 | 2.325 | 2.1 | 1.9 | 1.75 | 1.6 | 1.5 | 1.4 | 1.3 | 1.2 | 1.1 | 1 | 0.85 | 0.75 | 0.55 |
| Iteration 8 | 2.35 | 2.325 | 2.2 | 2.05 | 1.75 | 1.6 | 1.5 | 1.4 | 1.3 | 1.2 | 1.05 | 0.95 | 0.85 | 0.75 | 0.5 |
| Iteration 9 | 2.4 | 2.325 | 2.2 | 2.05 | 1.75 | 1.6 | 1.5 | 1.4 | 1.3 | 1.2 | 1.1 | 0.95 | 0.8 | 0.7 | 0.4 |
| Iteration 10 | 2.4 | 2.325 | 2.2 | 2.05 | 1.75 | 1.6 | 1.5 | 1.4 | 1.3 | 1.2 | 1.1 | 1 | 0.85 | 0.7 | 0.55 |

Figure 4.13 shows the comparison of flow rates of regular microchannel heat exchanger and tapered shape microchannel heat exchanger for each iteration. The result of analysis proved that the positioning of the channels in the microchannel heat

exchanger yielded more uniform flow distribution. When the iterations were compared with each other, it was observed that the first iteration flow rate had more uniform flow distribution than the other iterations. To make such a case clear, flow rate distribution of the channels in the first iteration is presented in Figure 4.14.

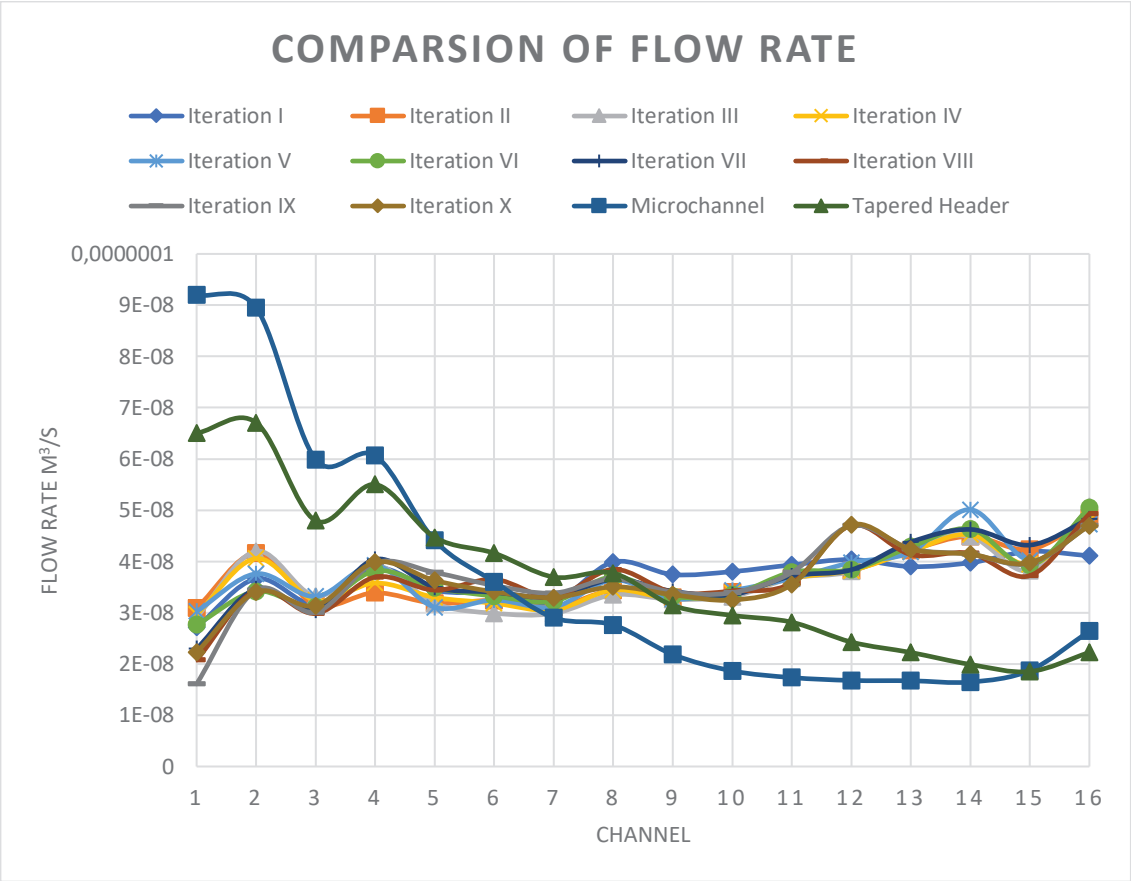


Figure 4.13. Comparison of the flow rate for all iterations

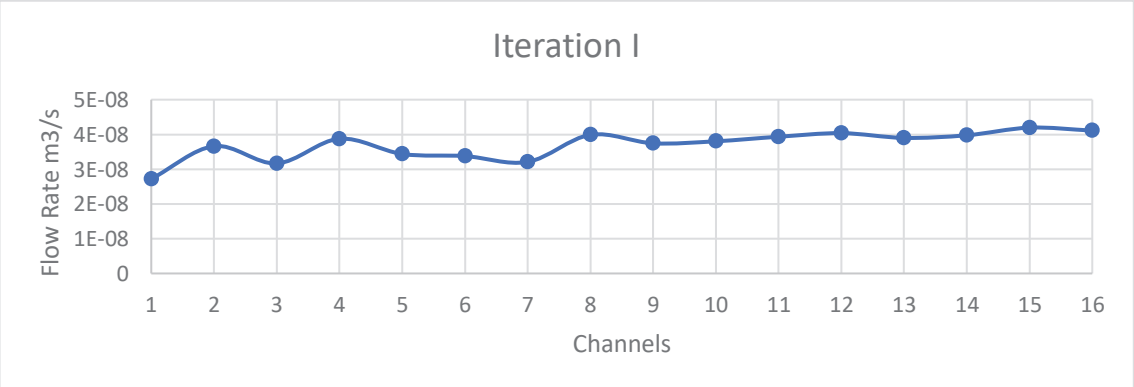


Figure 4.14. The first iteration flow rate

When the velocity distribution and temperature distribution were considered, the uniformity of fluid flow can be seen in Figure 4.15. The heat exchange was almost stable in all channels of the heat exchanger. At the last channel, the flow reached to expected temperature; thus, heat exchange was not observed in the proposed range of temperature.

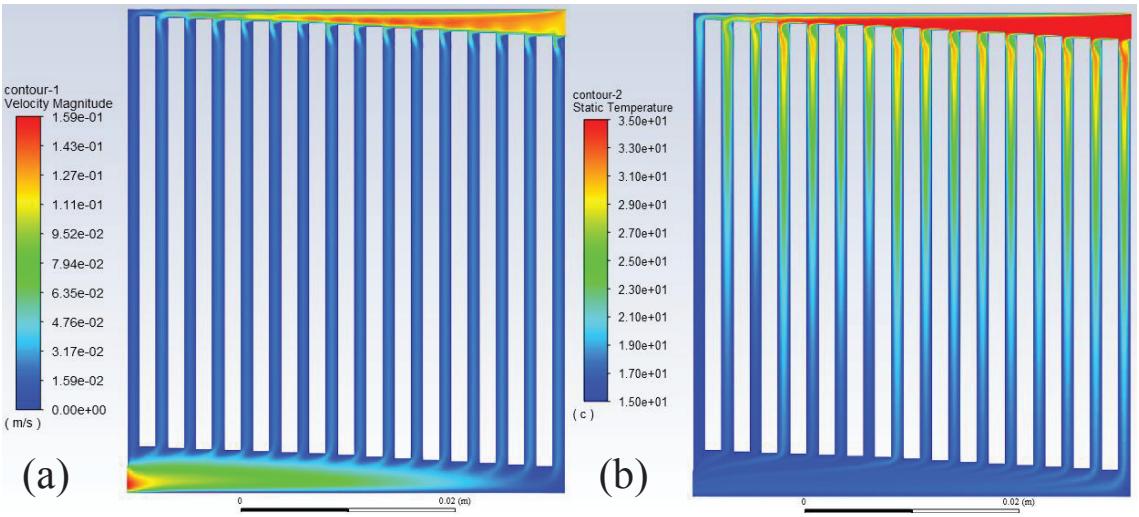


Figure 4.15. First iteration (a) Velocity profile (b) Static temperature distribution, RE=300

## 4.3 Two-Phase Flow Distribution with Improved Geometry

The two-phase flow regime and phase changing mechanism via condensing were already expressed in the previous chapter. Here, the two-phase flow distribution was investigated using improved geometry and it was observed that improved geometry reduced the maldistribution effects on flow distribution. Thus, refrigerant fluid R410a was worked on the improved design with the initial conditions (Table 4.2).

The latent heat value is normally higher than the sensible heat value. Therefore, the phase changing mechanism needs to more heat dissipation rate or more duration time at the lower heat differences. Approaching that behavior, in this study, there are two main parameters directly affect the phase change process in the condenser, which

are volume flow rate and heat flux. The inlet velocity value determines the flow rates, meanwhile, initial heat differences can be also defined as working conditions for condenser specify heat flux. The inlet velocity is also a parameter for the Reynolds number and Reynolds number has also contained the other thermodynamical properties. The results are given via Reynolds number.

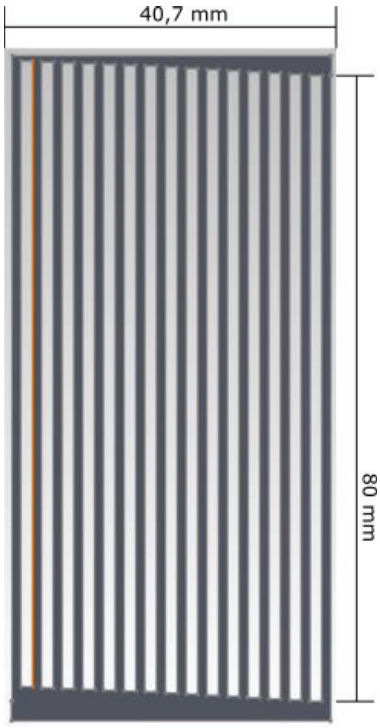


C

Figure 4.16 Design C for higher range of Reynolds number

Here, there were three different height designs that were designed to investigate which design was given a more reliable result for the high range Reynolds number. Design measurements are given in Table 4.3. According to table value, all designs had the same measurements except the channel height.

Table 4.2 Initial condition

| Initial Conditions | |
|---|---|
| Enthalpy | Value |
| $h_g$ (Superheated) 50°C | 484.4 kJ/kg |
| $h_l$ (Saturated Liquid) 20°C | 232 kJ/kg |

Table 4.3 Design measurements

| Design Measurements | | | |
|---|---|---|---|
| | A | B | C |
| Width | 40.7 | 40.7 | 40.7 |
| Height | 45 | 65 | 85 |
| Channels Quantities | 16 | 16 | 16 |
| Channels Heights | 40 | 60 | 80 |
| Square (mm2) | 932 | 1296 | 1660 |
| Calculated Heat Flux (kw/m2) | -0.05475 | -0.0393756 | -0.030741676 |

All value unit is mm

Due to the phase change mechanism, condensation needs more duration time. Doubled design provided more reliable results in the high range of Reynolds number. Considering the other design, A can be condensed only when the Reynolds number is 25 and lower. Similarly, B design was excused a little bit higher at 50 Reynolds number.

The results showed that the limit of 100% condensates A and B designs was reached. Only low Reynolds number or low heat flux values give the solution using R410a as a refrigerant fluid with these designs.

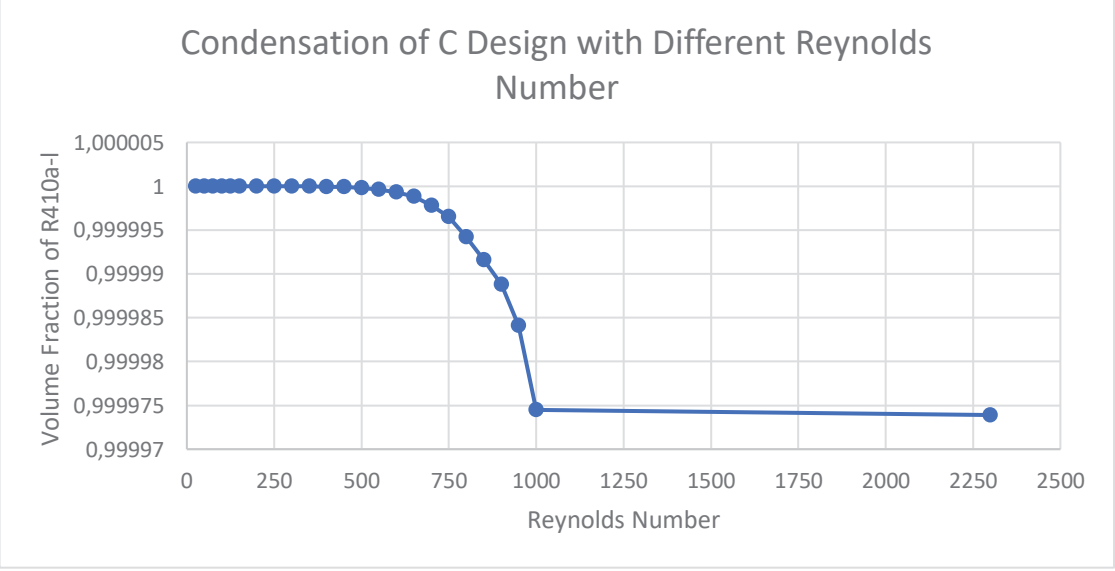


Figure 4.17 Condensation of C design with different Reynolds number

On the other hand, the C design can be solved in all Reynolds numbers in the limits of laminar flow. When considering the given result, the volume fraction value was 1 until the Reynolds number value 550 which meant that all of the refrigerant fluid condensated from vapor to liquid. After that, while the Reynolds number value was increasing, the volume fraction number was decreasing. Passing the 750 Reynolds number, the volume fraction was decreasing dramatically until the 1000 Reynolds number. After this value, R410a fluid was in the mixture form in the condenser.

As shown in In Figure 4.18, volume fraction contours of the R410a liquid phase are presented for different Reynold numbers. Red colors represent the R410a liquid phase, meanwhile blue colors show the vapor volume fraction. When the Reynolds number increased, the volume fraction value began to decrease after 550.

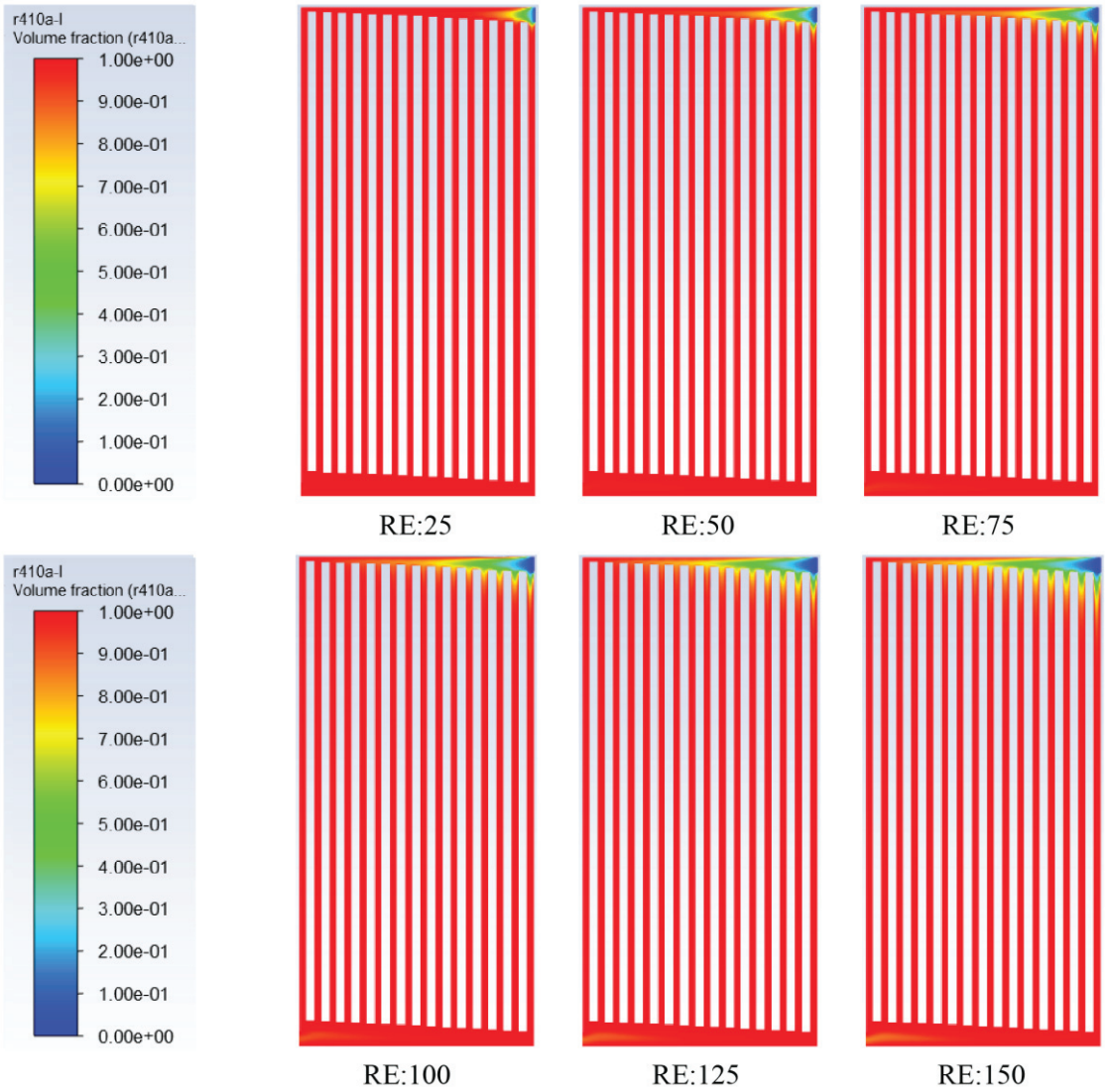

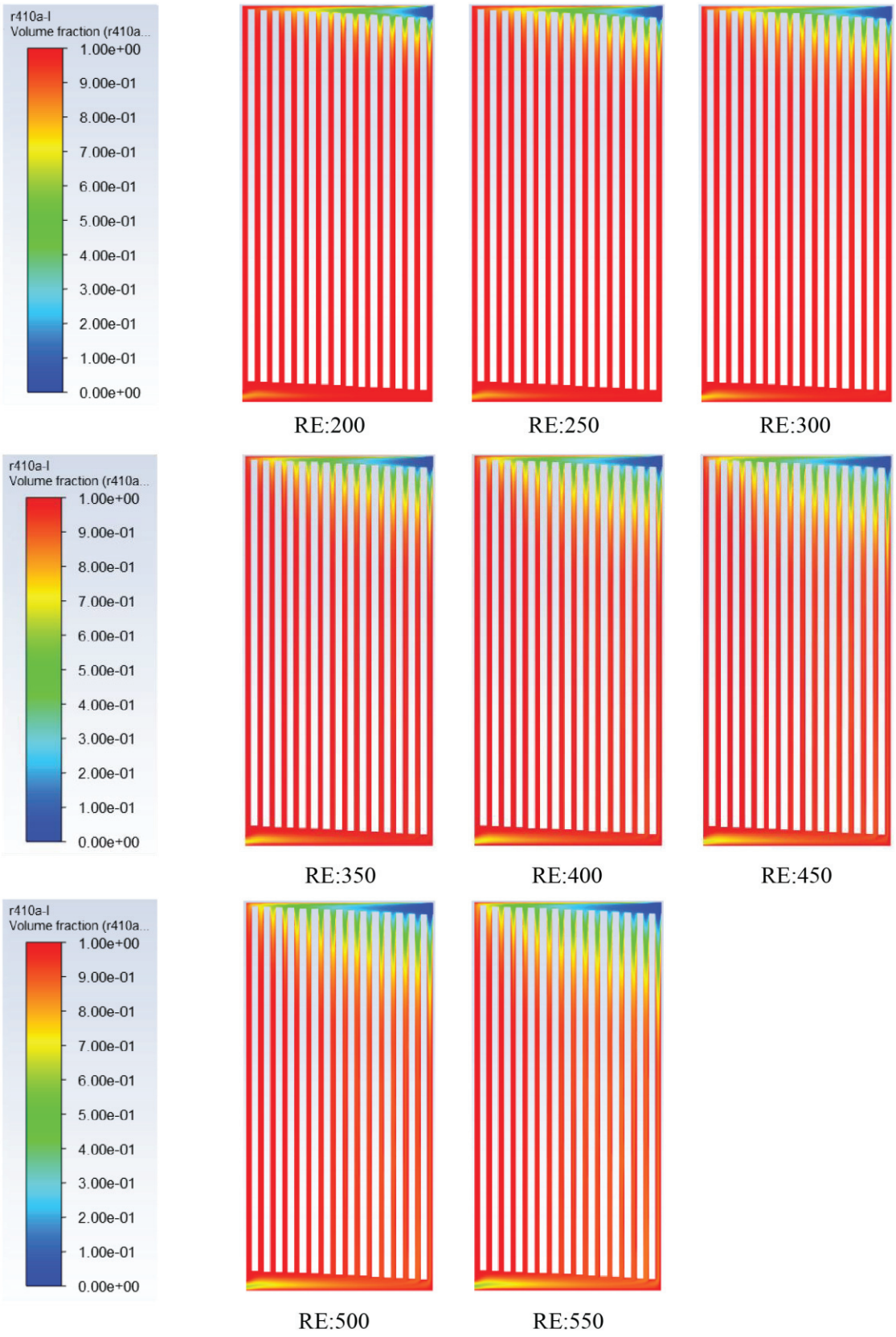


Figure 4.18 Volume fraction of R410a-liquid contour for various Reynolds number in design C

# CHAPTER 5

# CONCLUSION

This thesis documents the definition of maldistribution and how the effects of maldistribution on heat exchanger performance could be eliminated using improved geometries. In this thesis, first, the reference geometry of the microchannel was simulated. The simulation results were in agreement with reference geometry and literature. The temperature distribution and flow rate of the first geometry were nonuniform. Thus, to eliminate this uniformity, the first geometry was changed with the increased channel quantities and decreased channel dimensions to raise the thermal performance. After that, the flow distribution was analyzed and the geometrical improvements were applied to the microchannel heat exchanger. Such improvements included tapered header shape and channel protrusions in the header of the microchannel heat exchanger. To achieve a uniform flow, the header shape was transformed into a tapered shape. The flow distribution was then slightly uniformed. To make the flow even more uniform, the channels were repositioned in the header. The protrusion depth was determined iteratively. Ten iterations were performed and simulated under the same conditions of the microchannel heat exchanger. When the flow rates of the iterations were compared in this thesis, it was observed that the first iteration yielded more uniform flow distribution than the others. Then, the improved three designs were simulated with the refrigerant flow of R410a to investigate the phase-changing in the condenser. Channel height was increased to gain more heat transfer duration time. A and B designs condensed 100% the vapor phase of R410a only less than 75 Reynolds number. For C design, R410a was condensed 100% vapor phase to liquid phase till around Reynolds numbers 350. After the Reynolds number 350, the refrigerant fluid was mixture vapor and liquid phase. The volume fraction value decreased dramatically after the Reynolds number 1000. Overall, the maldistribution effect decreased with the repositioning of channels and protrusions. All in all, the thermal performance improved with all changes made on the geometry, and condensation was investigated with the different Reynolds number.

This study focused on the elimination of the maldistribution effects on flow distribution and performance of condenser. Different protrusion depths should be experimented in further studies to elucidate the effects of protrusion on the performance of the condenser better. New geometrical designs also should be applied to improve flow distribution and condensation.

# REFERENCES


A.Gogulakrishnanan, & M.Arun Pranesh. (2016, April). Numerical Analysis For Two Phase Flow Distribution Headers In Heat Exchangers. *International Journal of Scientific & Engineering Research, Volume 7-Issue 4*, 219-224.

Ahmad, M., Berthoud, G., & Mercier, P. (2009). General characteristics of two-phase flow distribution in a compact heat exchanger. *International Journal of Heat and Mass Transfer, 52*, 442-450.

Bajura, R., & Jones, E. (1976, December). Flow Distribution Manifolds. *J. Fluids Eng., 98*(4), 654-665. doi:10.1115/1.3448441

Bejan, A., & Lorente, S. (2010). The constructal law of design and evolution in nature. *Phil. Trans. R. Soc. B, 365*, 1335–1347. doi:10.1098/rstb.2009.0302

Brogan, R. (2011). Heat Exchangers. *THERMOPEDIA*. doi:10.1615/AtoZ.h.heat_exchangers

Cetkin, E. (2017). Constructal Microdevice Manifold Design With Uniform Flow Rate Distribution by Consideration of the Tree-Branching Rule of Leonardo da Vinci and Hess–Murray Rule. *JOURNAL OF HEAT TRANSFER, 139*. doi:10.1115/1.4036089

Cetkin, E., Lorente, S., & Bejan, A. (2010). Natural constructal emergence of vascular design with turbulent flow. *Journal of Applied Physics*, 107.

Dario , E., Tadrist, L., & Passos, J. (2013). Review on two-phase flow distribution in parallel channels with macro and micro hydraulic diameters: Main results, analyses, trends. *Applied Thermal Engineering, 59*, 316-355.

Dönmez, N., & Onbaşıoğlu, S. (2013). Two Phase Flow in Heat Exchanger Manifolds. *Engineer and Machinery, 54/645*, 14-27.

Fluent User's Guide. (2013, November). *Fluent User's Guide.* Accessed : March, 2021 Pmtpoli:http://www.pmt.usp.br/academic/martoran/notasmodelosgrad/ANSYS%20Fluent%20Users%20Guide.pdf

Freon. (2019, January). *freon-410a-si-thermodynamic-properties.* Accessed: March 2021 freon: https://www.freon.com/en/-/media/files/freon/freon-410a-si-thermodynamic-properties.pdf

Gas Servei Technical Data Sheet. *Technical data sheet-R-410A-Gas Servei S.A*. Accessed: November 10, 2020 Gas-Servei.

Ghiaasiaan, S. (2008). *Two-Phase Flow, Boiling and Condensation.* Cambridge: Cambridge University Press.

Gosreports. (2017, 07 19). *Global Heat Exchangers Market Expected To Reach $ 18.57 Billion By 2021 With A CAGR Of 6.89%.* Accessed: March 2021 Gosreports: http://www.gosreports.com/global-heat-exchangers-market/

Husain, A. (2016). A Review on Advances in Design and Development Of Heat Exchangers. *International Journal of Research and Scientific Innovation (IJRSI), Volume III*(Issue XI), 60.

Ishii, M., & Hibiki, T. (2011). *Thermo-Fluid Dynamics of Two-Phase Flow.* New York: Springer-Verlag New York. doi:10.1007/978-1-4419-7985-8

Jafar M. Hassan, & Thamer A. Mohamed. (2014). Modeling the Uniformity of Manifold with Various Configurations. (M. S. Mansour, Dü.) *Journal of Fluids*, 8. doi:10.1155/2014/325259

Jobson, M. (2014). *Energy Considerations in Distillation* (9780123865472 b.). Academic Press. doi:https://doi.org/10.1016/B978-0-12-386547-2.00006-5.

Kakaç, S., Hongtan, L., & Anchasa, P. (2012). *Heat Exchangers Selection, Rating and Thermal Design.* Boca Raton: CRC Press.

Kandlikar, S. G., & William J. Grande. (2003). Evolution of Microchannel Flow Passages-Thermohydraulic Performance and Fabrication Technology. *Heat Transfer Engineering, 24(1)*, 3–17. doi:10.1080/01457630390116077

Kandlikar, S., Garimella, S., Li, D., Colin, S., & King, M. (2006). *Heat Transfer and Fluid Flow in Minichannels and Microchannels.* Waltham: Elsevier Ltd. .

Kandlikar, Satish & Steinke, & Mark. (2003). Predicting Heat Transfer During Flow Boiling in Minichannels and Microchannels. *ASHRAE Transactions, 109*, 667-676.

Kim, S., Eunsoo Choi, & Young I. Cho. (1995). The Effect Of Header Shapes on the Flow Distribution in a Manifold For Electronic Packaging Applications. *International Communications in Heat and Mass Transfer*, 329-341.

Koyama, S., Wijayanta, A., Kuwahara, K., & Ikuta, S. (2006). Developing Two-Phase Flow Distribution in Horizontal Headers With Downward Minichannel-Branches. *International Refrigeration and Air Conditioning Conference* (s. 745-753). Indiana: Purdue e-Pubs. http://docs.lib.purdue.edu/iracc/745

Marchitto, A., Fossa, M., Guglielmini, G., & Paietta, E. (2014). Two-Phase Flow Distribution in Parallel Vertical Channels Fed By A Variable Depth Protrusion Header. *Multiphase Flow in Industrial Plants* (s. 1-12). Genova: Italian Association of Industrial Plant Engineering.

Mehendale S.S, Jacobi A.M., & Shah R.K. . (1999). Meso- and Micro-Scale Frontiers of Compact Heat Exchangers. *Applied Optical Measurements*, 139-158.

Minqiang, P., Dehuai, Z., Yong, T., & Dongqing, C. (2009). CFD-based Study of Velocity Distribution among Multiple Parallel Microchannels. *Journal Of Computers, 4*(11), 1133-1138.

Mueller, A., & Chiou, J. (1988). Review of various Types of Flow Maldistribution in Heat Exchangers. *Heat Transfer Engineering, 9:2*, 36-50. doi:10.1080/01457638808939664

*Multi-Phase Flows And Discrete Phase Modelled*. (2020, December). Accessed: December 2020 Cfdyna: http://cfdyna.com/Home/of_multiPhase.html

Pai, S. (1977). *Introduction: Classification of Two-Phase Flows. In: Oswatitsch K. (eds) Two-Phase Flows.* Springer Fachmedien Wiesbaden. doi:10.1007/978-3-322-86348-5_1

Panghat, K., & Mehendale, S. (2016). A Critical Assessment of Two-Phase Flow Distribution in Microchannel Heat Exchangers. *International Refrigeration and Air Conditioning Conference*, 1597. http://docs.lib.purdue.edu/iracc/1597

Prescient&Strategic Intelligence. (2016, January). *Heat Exchangers Market Size Global Forecast Report 2020*. Accessed: March 19, 2021 PS Market Research : https://www.psmarketresearch.com/market-analysis/heat-exchangers-market

Ronquillo, R. (2020). *Understanding Heat Exchangers.* Accessed: December 2020 tarihinde thomasnet: https://www.thomasnet.com/articles/process-equipment/understanding-heat-exchangers/

Shi, J., Qu, X., Qi, Z., & Chen, J. (2011). Investigating performance of microchannel evaporators with different manifold structures. *International Journal of Refrigeration*, 292-302. doi:10.1016/j.ijrefrig.2010.08.008

Silva, A., Lorente, S., & Bejan, A. (2004). Optimal distribution of discrete heat sources on a plate with laminar forced convection. *International Journal of Heat and Mass Transfer, 47*, 2139-2148. doi:10.1016/j.ijheatmasstransfer.2003.12.009

Swift, G., Migliori, A., & John, W. (1985). Construction of and Measurements with an Extremely Compact Cross-Flow Heat Exchanger. *Heat Transfer Engineering, 6*(2), 39-47.

Tong , J., Sparrow , E., & Abraham , J. (2009). Geometric strategies for attainment of identical outflows through all of the exit ports of a distribution manifold in a manifold system. *Applied Thermal Engineering, 29*, 3552-3560. doi:10.1016/j.applthermaleng.2009.06.010

Tuckerman, D., & Pease, R. (1981). High-Performance Heat Sinking for VLSI. *IEEE Electron Device Letters, Vol. Edl-2*(No. 5), 126-129.

Tuo, H., & Hrnjak , P. (2013). Effect of the header pressure drop induced flow maldistribution on the microchannel evaporator performance. *International Journal Of Refrigeration, 30*, 2176-2186.

Vist, S., & Pettersen, J. (2004). Two-phase Flow Distribution in Compact Heat Exchanger Manifolds. *Experimental Thermal and Fluid Science, 28*, 209–215.

Wang, C.-C., Yang, K.-S., Tsai, J.-S., & Chen, I. (2011). Characteristics of Flow Distribution in Compact Parallel Flow Heat Exchangers, Part I: Typical inlet header. *Applied Thermal Engineering*, 3226-3234. doi:10.1016/j.applthermaleng.2011.06.004

Wang, C.-C., Yang, K.-S., Tsai, J.-S., & Chen, I. (2011). Characteristics of Flow Distribution in Compact Parallel Flow Heat Exchangers, Part II: Modified Inlet Header. *Applied Thermal Engineering, 31*, 3235-3242. doi:10.1016/j.applthermaleng.2011.06.003

Webb, R., & Chung, K. (2005). Two-Phase Flow Distribution to Tubes of Parallel Flow Air-Cooled Heat Exchangers. *Heat Transfer Engineering*, 3-18. doi:10.1080/01457630590916239

Yanhui Han, Yan Liu, Ming Li, & Jin Huang. (2012). A Review of Development of Micro-Channel Heat Exchanger Applied in Air-Conditioning System. *Energy Procedia, 14*, 148-153.

# APPENDIX A

## P-H DIAGRAM REFRIGERANT R-410A